



# LIVE LOAD DISTRIBUTION FACTORS FOR WASHINGTON STATE SR 18/SR516 OVERCROSSING

WA-RD 477.1

Research Report  
February 2000



**Washington State  
Department of Transportation**

Washington State Transportation Commission  
Planning and Programming Service Center  
in cooperation with the U.S. Department of Transportation  
Federal Highway Administration



## TECHNICAL REPORT STANDARD TITLE PAGE

1. REPORT NO. WA-RD 477.1	2. GOVERNMENT ACCESSION NO.	3. RECIPIENT'S CATALOG NO.
4. TITLE AND SUBTITLE Live Load Distribution Factors for Washington State SR 18/SR 516 Overcrossing		5. REPORT DATE February 2000
7. AUTHOR(S) Paul Barr, John Stanton, Marc Eberhard		6. PERFORMING ORGANIZATION CODE
9. PERFORMING ORGANIZATION NAME AND ADDRESS Washington State Transportation Center (TRAC) University of Washington, Box 354802 University District Building; 1107 NE 45th Street, Suite 535 Seattle, Washington 98105-4631		8. PERFORMING ORGANIZATION REPORT NO.
12. SPONSORING AGENCY NAME AND ADDRESS Research Office Washington State Department of Transportation Transportation Building, MS 47370 Olympia, Washington 98504-7370 Keith Anderson, Project Manager, 360-709-5405		10. WORK UNIT NO.
13. TYPE OF REPORT AND PERIOD COVERED Research Report		11. CONTRACT OR GRANT NO. Agreement T9903, Task 73
15. SUPPLEMENTARY NOTES This study was conducted in cooperation with the U.S. Department of Transportation, Federal Highway Administration.		14. SPONSORING AGENCY CODE
16. ABSTRACT <p style="text-align: justify;">                     This report presents an evaluation of live-load distribution factors for a series of three-span, prestressed concrete girder bridges. The response of one bridge, measured during a static live-load test, was used to evaluate the reliability of a finite-element model. Twenty-four variations of this model were then used to evaluate the procedures for computing live-load distribution factors that are embodied in three bridge design codes. The finite-element models were also used to investigate the effects that lifts, intermediate diaphragms, end diaphragms, continuity, skew angle and load type have on distribution factors. For geometries similar to those considered in the development of the American Association of State Highway and Transportation Officials (AASHTO) Load and Resistance Factor Design (LRFD) Specifications (1994), the distribution factors computed with the finite-element models were within 6 percent of the code values. However, for the geometry of the bridge that was tested, the discrepancy was 28 percent. Lifts, end diaphragms, skew angle and load type significantly decreased the distribution factors, while continuity and intermediate diaphragms had the least effect. If the bridge had been designed using the distribution factors calculated with the finite-element model rather than the code values, the required concrete release strength could have been reduced by 6.9 Mpa (1000 psi), or the live load could have been increased by 39 percent.                 </p>		
17. KEY WORDS Live-load distribution, skew, diaphragms, continuity, lifts	18. DISTRIBUTION STATEMENT No restrictions. This document is available to the public through the National Technical Information Service, Springfield, VA 22616	
19. SECURITY CLASSIF. (of this report) None	20. SECURITY CLASSIF. (of this page) None	21. NO. OF PAGES 86
		22. PRICE



**Final Research Report**  
Research Project T9903, Task 73  
High Performance Concrete in Bridge Girders

**LIVE LOAD DISTRIBUTION FACTORS FOR  
WASHINGTON STATE  
SR 18/SR 516 OVERCROSSING**

by

Paul Barr  
Ph.D. Candidate

John Stanton, Ph.D.  
Professor

Marc Eberhard, Ph.D.  
Associate Professor

Department of Civil Engineering  
University of Washington  
Seattle, Washington 98195

**Washington State Transportation Center (TRAC)**  
University of Washington, Box 354802  
University District Building  
1107 NE 45th Street, Suite 535  
Seattle, Washington 98105-4631

Washington State Department of Transportation  
Technical Monitor  
Jerry Weigel  
Bridge and Structures Engineer

Prepared for

**Washington State Transportation Commission**  
Department of Transportation  
and in cooperation with  
**U.S. Department of Transportation**  
Federal Highway Administration

February 2000



## DISCLAIMER

The contents of this report reflect the views of the authors, who are responsible for the facts and the accuracy of the data presented herein. The contents do not necessarily reflect the official views or policies of the Washington State Transportation Commission, Department of Transportation, or the Federal Highway Administration. This report does not constitute a standard, specification, or regulation.

*PROTECTED UNDER INTERNATIONAL COPYRIGHT  
ALL RIGHTS RESERVED*  
NATIONAL TECHNICAL INFORMATION SERVICE  
U.S. DEPARTMENT OF COMMERCE

Reproduced from  
best available copy.





## TABLE OF CONTENTS

<b>CHAPTER 1: INTRODUCTION .....</b>	<b>1</b>
1.1 Context .....	1
1.2 Live Load Distribution Factors .....	1
1.3 SR 18/SR 516 Overcrossing .....	3
1.4 Research Objectives .....	4
1.5 Organization of Report.....	5
<b>CHAPTER 2: PREVIOUS RESEARCH.....</b>	<b>6</b>
2.1 Lin and Vanhorn (1968).....	6
2.2 Sithichaikasem and Gamble (1972) .....	6
2.3 Bakht and Jaeger (1985) .....	7
2.4 Khaleel and Itani (1990) .....	7
2.5 Zokaie, Ostserkamp and Imbsen (1991) .....	7
2.6 Chen and Aswad (1996):.....	10
2.7 Ebeido and Kennedy (1996) .....	11
2.8 Mabsout, Tarhini, Frederick and Tayar (1997).....	12
2.9 Summary .....	13
<b>CHAPTER 3: LIVE-LOAD TEST.....</b>	<b>15</b>
3.1 Bridge Description .....	15
3.2 Instrumentation .....	18
3.3 Description of Truck .....	20
3.3 Truck Placement .....	20
<b>CHAPTER 4: FINITE ELEMENT MODEL.....</b>	<b>23</b>
4.1 Modeling Strategy .....	23
4.1.1 Selection of Topology and Model Elements.....	23
4.1.2 Modeling of Girders.....	25
4.1.3 Modeling of Deck, Lift and Diaphragms .....	29
4.1.4 Constraints .....	30
4.2 SR 18/SR 516 Overcrossing .....	31
4.3 Single Span Bridge.....	32
4.4 Variations in Model Geometry .....	32
4.5 Loading .....	32
4.6 Calculated Moments .....	33
<b>CHAPTER 5: EVALUATION OF ANALYTICAL MODEL .....</b>	<b>35</b>
5.1 Measured Moment .....	35

5.2 Midspan Loading .....	36
5.3 Influence Line .....	40
5.4 Finite Element Model: Summary and Conclusion .....	40
<b>CHAPTER 6: LIVE LOAD DISTRIBUTION FACTORS .....</b>	<b>43</b>
6.1 Code Live Load Distribution Factors .....	43
6.1.1 AASHTO LRFD Specification Factors .....	44
6.1.2 AASHTO Standard Specification Factors .....	46
6.1.3 OHBDC Factors .....	47
6.2 Finite Element Models .....	50
6.3 Loading Scheme .....	51
6.4 Evaluation of Code Live Load Distribution Factors—Truck Loading .....	53
6.4.1 Comparison of Code LLDFs with those Derived from FEM Analysis .....	54
6.4.2 Effects of Lifts .....	57
6.4.3 Effects of Intermediate Diaphragms .....	59
6.4.4 Effects of End Diaphragms .....	61
6.4.5 Effects of Continuity .....	64
6.4.6 Comparison of Effects .....	66
6.4.7 Effect of Skew .....	69
6.5 Evaluation of Code Live Load Distribution Factors—Lane Loading .....	71
<b>CHAPTER 7: DESIGN IMPLICATIONS .....</b>	<b>74</b>
<b>CHAPTER 8: CONCLUSIONS AND RECOMMENDATIONS .....</b>	<b>78</b>
8.1 Static Live Load Test .....	78
8.2 Comparison with Codes .....	79
8.3 Influences on the Live Load Distribution Factors .....	80
8.3.1 Effect of Lifts .....	80
8.3.2 Effect of Intermediate Diaphragms .....	81
8.3.3 Effect of End Diaphragms .....	81
8.3.4 Effect of Continuity .....	81
8.3.5 Effect of Skew .....	82
8.3.6 Effect of Lane Loading .....	82
8.4 Design Implications .....	83
8.5 Research Recommendations .....	83
<b>REFERENCES .....</b>	<b>84</b>

## LIST OF FIGURES

<u>Figure</u>		<u>Page</u>
3.1	Bridge Layout .....	16
3.2	Bridge Cross-Section at Pier 2 (looking north).....	16
3.3	W74MG Girder Dimensions .....	17
3.4	Intermediate Diaphragms .....	18
3.5	Instrumentation Sites in HPC Bridge.....	19
3.6	Cross-Section of Typical Instrumentation Site .....	20
3.7	Truck Axle Loads and Dimensions .....	21
3.8	Truck Locations for Readings .....	22
4.1	Cross-Section of Finite Element Model of Two Girders .....	25
4.2	Comparison of Differential Equation and FEM Solution .....	28
4.3	Notation for Shape Function Definition.....	33
5.1	Midspan Response Due to Midspan Loading .....	38
5.2	Comparison of Midspan Moment from FEM Model and VWSGs...	39
5.3	Influence Lines for Midspan Moment .....	41
6.1	OHBDC Three-Lane Bridge Live Load Distribution Coefficient Chart	49
6.2	Example Loading Scheme for Two-Lane Loading .....	52
6.3	Distribution Factors for Truck Loading .....	56
6.4	Effect of Lifts .....	58
6.5	Effect of Intermediate Diaphragms .....	60
6.6	Fixed-Fixed Beam with a Skew Angle $\alpha$ .....	61
6.7	Effect of End Diaphragms.....	63
6.8	Effect of Continuity .....	65
6.9	Combined Effects .....	68
6.10	Effect of Skew .....	70
6.11	Distribution Factors for the AASHTO Truck and Lane Loading .....	73
7.1	Design Implications for Live Load Distribution Factors .....	77

## LIST OF TABLES

<u>Figure</u>		<u>Page</u>
3.1	Section Properties .....	17
4.1	Properties for Girder Element .....	29
4.2	Deck, Lift and Diaphragm Properties .....	30
4.3	SR 18/SR 516 Column Properties .....	31
8.1	Ratio of Model 5 and Code Distribution Factors .....	79
8.2	Ratio of Model 1 and Code Distribution Factors .....	80

# CHAPTER 1 INTRODUCTION

## 1.1 CONTEXT

Precast, prestressed concrete girder bridges are often more economical to construct and maintain than other types of bridges. The economy of such bridges promises to increase with the introduction of improved materials, such as high-performance concrete (HPC), and larger diameter, low-relaxation prestressing strands (Goodspeed et al., 1996). Larger sections will further increase the spans that can be achieved and thus the range of application of precast-prestressed concrete girder bridges (Seguirant, 1998). Further efficiencies could be realized if current design procedures (e.g., AASHTO Standard Specifications (1996), AASHTO LRFD (1994)) were less conservative.

This report provides the results of a field and analytical investigation of the live-load distribution behavior of a particular bridge. The approximation of the bridges' actual behavior with code live-load distribution factors is one aspect of design that may be too conservative (Chen and Aswad, 1996). The purpose of this study was to investigate the accuracy with which live-load moments are approximated with existing code procedures.

## 1.2 LIVE-LOAD DISTRIBUTION FACTORS

Live load distribution factors allow engineers to analyze bridge response by treating the longitudinal and transverse effects of wheel loads as uncoupled phenomena. These factors have simplified the design process by allowing engineers to calculate the girder design moment as the static moment caused by a truck load multiplied by a

live-load distribution factor. A low distribution factor arises when the bridge shares the load efficiently among neighboring girders, and leads to a low design moment for a given truck size.

The Standard Specification for Highway Bridges has contained live load distribution factors since 1931. The early values were based on the work by Westergaard (1930) and Newmark (1948), and they have been updated and modified as new research results became available. For a bridge constructed with a concrete deck on prestressed concrete girders and carrying two or more lanes of traffic, the current distribution factor (AASHTO Standard Specifications, 1996) is  $S/5.5$ , where  $S$  is the girder spacing in feet. This factor is applied to the moment caused by one line of wheels. However, some researchers (Zokaie et al., 1991) have noted that the changes that have taken place over the last 55 years have led to inconsistencies in the load distribution criteria in the Standard Specifications. These inconsistencies include:

- inconsistent consideration of a reduction in load intensity for multiple lane loading
- inconsistent changes in distribution factors to reflect changes in design lane width
- inconsistent verification of accuracy of wheel load distribution factors for various bridges.

In addition to these inconsistencies, the distribution factors in the Standard Specification were developed considering only simply supported bridges with no skew (Newmark, 1948). Despite these limitations of the initial study, the current Standard Specification states that the distribution factors can be applied to the design of normal highway bridges. The Standard Specifications do not, however, state what constitutes a normal highway bridge.

In 1994, AASHTO adopted the LRFD Bridge Design Specifications (AASHTO, 1994) as an alternative to the Standard Specifications. The LRFD Specifications recommend new load distribution equations. These distribution formulas resulted from National Cooperative Highway Research Program research project 12-26, reported by Zokaie et al. (1991). The formulas take into account many more bridge parameters than were previously considered, including skew and continuity. According to Zokaie et al. (1991), the new distribution factors lie within 5 percent of the actual distribution factors found by analyzing the bridge decks with a detailed finite element model.

Although the AASHTO LRFD equations for the distribution factors are believed to be more accurate than the distribution factors in the Standard Specifications, some researchers (e.g. Chen and Aswad, 1996) have found that they can be uneconomically conservative for bridges with large span-to-depth ratios. Chen and Aswad (1996) found that this conservatism can be as much as 18 to 23 percent for interior beams and 4 to 12 percent for exterior beams. A reduction in this conservatism could lead to more economical designs or to an increase in the span that can be achieved with a given girder size.

Research is needed to evaluate the conservatism of current design procedures.

### **1.3 SR18/SR516 OVERCROSSING**

The Federal Highway Administration (FHWA) has been encouraging state departments of transportation to use HPC in bridge applications because of its potential benefits in terms of versatility, through longer spans or, shallower sections, or of economy, through the use of fewer, stronger, girders. Since the Washington State

Department of Transportation (WSDOT) was also interested in expanding the use of HPC to structural applications, WSDOT designed a new HPC bridge to carry the eastbound lanes of State Route 18 (SR 18) over SR 516. The bridge (Barr et al., 1998) has three spans with lengths of 24.4 m, 41.7 m and 24.4 m (80 ft, 137 ft and 80 ft) respectively. The girders were designed to have a concrete strength at release of 51 MPa (7,400 psi) and 68.9 MPa (10,000 psi) at 56 days. As a result of specifying HPC, the WSDOT was able to reduce the number of lines of girders from seven to five.

The roadway deck has a width of 11.6 m (38 ft) and a thickness of 190 mm (7.5 in.). The design compressive strength of the deck concrete is only 27.6 MPa (4000 psi), but it has enhanced durability properties due to the use of fly ash and the requirement of a 14-day water cure. The SR18/SR516 overcrossing is described further in Chapter 3.

The bridge girders were heavily instrumented in order to study their long-term behavior. The presence of the instrumentation provided the opportunity to conduct a live-load test at a low incremental cost. That test constitutes the experimental component of this study.

#### **1.4 RESEARCH OBJECTIVES**

The overall objective of the study was to evaluate the accuracy with which the live load distribution factors in the AASHTO LRFD specifications represents the actual load distribution in bridges similar to the SR18/SR516 overcrossing. The study considered distribution factors for flexure but not for shear. Detailed goals included the evaluation of the effects on live load distribution of lifts (which is the volume of concrete cast between the girder and deck to compensate for camber), diaphragms, continuity and skew angle. This evaluation was conducted by performing the following tasks:

1. Measuring the responses of the SR18/SR516 overcrossing to a 35-kip truck placed at numerous locations.
2. Comparing the measured response of the bridge with the response calculated from a finite element model. The model accounted for the effects of the columns, pier caps, deck, lifts, intermediate diaphragms and end diaphragms.
3. Evaluating the effect of lifts, diaphragms, continuity, and skew on the load distribution factors for the bridge by means of an analytical parameter study, using the Finite Element Model that had been verified against experimental data in Task 2.

## **1.5 ORGANIZATION OF REPORT**

This report is organized as follows:

- Chapter 2 describes previous research.
- Chapter 3 describes the bridge construction and the field testing.
- Chapter 4 describes the development of the finite element model.
- Chapter 5 describes the evaluation of the finite element model by comparing its results with the measured behavior of the bridge.
- Chapter 6 evaluates the effects of skew, continuity, lifts and diaphragms on the load distribution.
- Chapter 7 discusses the impact that the findings of this report have on the design of the SR18/SR516 precast prestressed concrete bridge girders.
- Chapter 8 summarizes the conclusions of the report. Recommendations for future research are also made.

## **CHAPTER 2 PREVIOUS RESEARCH**

Other researchers have investigated the effects of skew, continuity and diaphragms on live-load distribution in bridges. This chapter summarizes some of this research.

### **2.1 LIN AND VANHORN (1968)**

This study was the fifth in a series of five studies that was sponsored by the Pennsylvania Department of Transportation and the Federal Highway Administration to investigate the load distribution in prestressed concrete box-beam bridges. This study focused primarily on the field testing of a bridge with and without midspan diaphragms. The effect of midspan diaphragms on load distribution was evaluated.

The researchers found that when one truck was placed on the bridge, the distribution coefficients and the deflections of the girders were reduced slightly by diaphragms. However, when multiple lanes were loaded, the midspan diaphragms had nearly no effect on the distribution coefficients (Lin and VanHorn, 1968).

### **2.2 SITHICHAIKASEM AND GAMBLE (1972)**

Sithichai Kasem and Gamble (1972) were among the first researchers to study the effects of intermediate diaphragms in prestressed concrete bridges. The solution to various bridge configurations were found using Fourier series solutions. The series solution included material properties, section properties, flexural stiffness, torsional stiffness and warping stiffness. The following conclusions were reached:

- The addition of intermediate diaphragms may not reduce the maximum girder moment and may even cause slight increases in some cases. When intermediate

diaphragms are added to bridges with spans exceeding 70 ft, no reduction or a slight increase in girder moment may occur. For bridges with spans smaller than 70 ft, intermediate diaphragms may reduce the girder moment. For all bridges, no major reduction in moment occurred when intermediate diaphragms were added.

- Intermediate diaphragms only caused a measurable change in girder moment when the diaphragm was placed at or near the section of maximum moment.
- The intermediate diaphragm must have the correct flexural stiffness for any benefit to occur. If the flexural stiffness of the intermediate diaphragm is too large, an increase in maximum girder moment can occur.

### **2.3 BAKHT AND JAEGER (1985)**

This research provided much of the basis for the live load distribution procedures given in the Ontario Highway Bridge Design Code (1992). The approach used was to treat the bridge as an anisotropic plate, with properties given by the smeared stiffnesses of the true structure. From these equivalent plate properties, torsion and flexural parameters,  $\alpha$  and  $\theta$ , are computed. Live load distribution factors are then obtained as functions of  $\alpha$  and  $\theta$  from design charts, and girder design moments are given by the truck moment multiplied by the distribution factor.

According to this method is applicable to shallow bridges. The design charts that were developed to obtain the load distribution factors were developed for unskewed, simply supported bridges. The method can be applied to continuous bridges by taking the span length as the length between inflection points.

## **2.4 KHALEEL AND ITANI (1990)**

Khaleel and Itani (1990) evaluated the behavior of continuous slab-on-girder bridges with varying degrees of skew subjected to the AASHTO HS20-44 loading. A total of 112 continuous bridges with five pretensioned girders were analyzed using the finite element method. The span lengths varied between 24.4 and 36.6 m (80 and 120 ft), and the skew was varied between 0 and 60°. The girder spacings were between 1.8 and 2.7 m (6 and 9 ft).

The researchers found that the AASHTO Standard Specifications underestimated the positive bending moment for exterior girders by as much as 28 percent. They also concluded that, in some cases, the AASHTO Standard Specifications underestimated the design moment for an interior girder by 6 percent. Other cases resulted in the design moment for an interior girder being overestimated by as much as 40 percent.

The skew angle was found to significantly reduce the design moment. If the skew angle was less than 30°, the reduction in both positive and negative moments was less than 6 percent for interior girders. In contrast, if the skew angle was 60°, the design moment was reduced by as much as 29 percent for the same interior girder. For exterior girders, the reduction of the maximum positive or negative moments was less than 10 percent for skew angles less than 45° and as much as 20 percent when the skew angle was 60°.

## **2.5 ZOKAIE, OSTERKAMP AND IMBSEN (1991)**

This study, which was funded by the National Cooperative Highway Research Program (NCHRP) (Project 12-26), focused on evaluating and developing methods for computing live-load distribution factors for commonly used bridge types. The study

considered slab-on-beam bridges; multi-cell, box-girder bridges; slab bridges; multi-box beam bridges; and spread box beam bridges. Three methods of analysis were used to investigate the live load distribution factors for each bridge type.

- Level 3, which was considered the most accurate analysis, included calculating the live-load distribution factors with a detailed finite element modeling of the bridge deck. A variety of finite-element programs were used to analyze the bridges. In the case of slab-on-beam bridges, shell elements were used to model the deck, and beam elements, in a different plane than the shell elements, were used to model the girders.
- Level 2 analysis included the use of nomographs, design charts and grillages using grid models to calculate the live load distribution factors.
- Level 1 analysis used simplified formulas, based on Level 2 and 3 analyses, to calculate the live-load distribution factors. These formulas were evaluated and found to have similar levels of accuracy as the Level 2 and 3 analysis for their ranges of applicability. Correction factors were applied to the formulas to account for the effect of girder location (edge or interior), skew and continuity.

For each type of bridge investigated, Level 3 analysis was performed on an “average bridge.” This “average bridge” was a theoretical bridge made of the average bridge properties (beam spacing, span length, slab thickness, etc.) of a pool of random bridges from a number of states (Zokaie et al., 1991).

The sensitivity of the live-load distribution factors to various bridge properties was also investigated. Bridge properties of the average bridge were varied one at a time, and their effect on the distribution factors was analyzed. Beam spacing was determined

to be the most significant property, but span length, longitudinal stiffness, and transverse stiffness also affected the distribution factors. The formulas derived in the Level 1 analysis were obtained by fitting power curves to results obtained from Levels 2 and 3 analyses.

According to the Zokaie et al., this research resulted in formulas (Level 1 analysis) for predicting live-load distribution that are more accurate than those used in the previous codes. These formulas are simpler, easier to use and nearly as accurate when compared with the methods from the Level 2 and 3 analysis. In addition, recommendations were made for the use of computer programs to calculate distribution factors (Zokaie et al., 1991).

## **2.6 CHEN AND ASWAD (1994, 1996)**

The main objective of this study was to review the accuracy of the formulas for live load distribution for flexure contained recommended in the LRFD Specification (AASHTO 1994) for modern prestressed concrete bridges made of I-girders or spread box girders with high span-to-depth ratios. The researchers felt that the average span of 20.0 m (65.5 ft) used in developing the LRFD equations did not accurately represent the span lengths that would be used in future design.

Chen and Aswad (1996) investigated ten simply supported bridge superstructures with span lengths varying from 27.4 to 42.7 m (90 to 140 ft). Girder spacing varied between 2.4 and 3.1 m (8 and 10 ft), and the total width of the bridge was either 16.6 or 18.3 m (48 or 60 ft). A 10-inch thick intermediate diaphragm was placed at midspan of the bridge. The top of the intermediate diaphragm began 6 inches below the bottom of the deck and the bottom ended 21-inches above the bottom of the girder. Finite element

analyses showed that the distribution factors for these bridges were 18 to 23 percent smaller for an interior girder and 4 to 12 percent smaller for an exterior girder than those computed with the procedures in the LRFD code.

A sensitivity study was also performed on certain geometric and material properties of the bridge to investigate their impact on the distribution factors. It showed that changing the load from an HS-20 truck to an LRFD HL-93 load changed the distribution factors for both exterior and interior girders by less than 1 percent. A 10 percent reduction in span length (from 42.7 m to 38.4 m (140 ft to 126 ft)) increased the distribution factors for both interior and exterior girders by only 1 percent.

Also, the authors showed in another paper (Aswad and Chen, 1994) that the percent reduction in distribution factor was approximately twice the corresponding reduction in prestressing strand or required concrete strength at release. For example, a 20 percent reduction in the distribution factors would generally lead to a 10 percent reduction in the required release strength or quantity of prestressing strand.

## **2.7 EBEIDO AND KENNEDY (1996)**

These researchers presented the results of a parametric study on two-span continuous composite steel-concrete bridges. This study considered more than 600 bridges. The parameters varied included girder spacing, skew, bridge aspect ratio, span ratio, number of lanes, number of girders and intermediate transverse diaphragms. In addition to varying the bridge properties, two loading cases were considered, namely, a partially loaded condition where trucks were only placed in certain lanes and a fully loaded condition where trucks were placed in every lane. The trucks were moved

transversely in their respective lanes in order to maximize the moment in the exterior and interior girders. Some of the conclusions of the study were:

1. The exterior girder controlled the design for both the span and support moments. For one and two lane bridges, the critical loading condition was the full truck loading. Bridges that had three or more lanes had to be investigated with both the partial and full loading conditions to determine the maximum moments for design.
2. Both the midspan and end moments decreased with increasing skew. This effect became more pronounced at angles greater than  $30^\circ$ .
3. The moment distribution factor was sensitive to girder spacing.
4. For bridges with skew angles greater than  $30^\circ$ , both span and support moments decreased significantly with increase in the span ratio (long span length/short span length).
5. Intermediate transverse diaphragms enhanced the load distribution characteristics of the bridge. An increase in the rigidity ratio,  $R$  (=transverse rigidity/longitudinal rigidity), increases the moment-distribution factor. Beyond a value of  $R=20$ , no increase in the factor occurred.

## **2.8 MABSOUT, TARHINI, FREDERICK AND TAYAR (1997)**

Mabsout, Tarhini, Frederick, and Tayar (1997) compared the performance of four finite element-modeling techniques that had been used by other researchers to evaluate the wheel load distribution factors of slab on girder bridges. A simply supported, two-lane, composite bridge of typical dimensions was analyzed with each of these four models. An AASHTO HS20-44 design truck load was applied to each model, and the

results were compared with the load distribution factors predicted in the LRFD Bridge Design Specifications (AASHTO 1994) and the Standard Specifications for Highway Bridges (AASHTO 1996). The four finite element models produced results that were similar to the distribution factors predicted by AASHTO LRFD formula, but not with the distribution factors predicted by methods given in the Standard Specifications for Highway Bridges (1996).

In addition to the finite element comparisons, the distribution factors from the AASHTO LRFD and the AASHTO Standard Specifications were compared with distribution factors measured from field tests performed by other researchers. Again, the AASHTO LRFD distribution factors correlated well with measured distribution factors, whereas the AASHTO Standard Specifications distribution factors were up to 27 percent conservative.

## **2.8 SUMMARY**

The aforementioned research can be summarized as follows:

- There appears to be a consensus that the Standard Specifications (AASHTO, 1996) are very conservative, and ignore many parameters such as skew (Mabsout et al., 1997) (Khaleel and Itani, 1990).
- The distribution factors predicted with the AASHTO LRFD may be conservative, especially for spans longer than those used in the Zokaie et al. study (Chen and Aswad, 1996).
- Skew reduces design moments, particularly for interior girders (Khaleel and Itani, 1990) (Ebeido and Kennedy, 1996).

- The effects of continuity are not clear but seem to increase the midspan moment. Using the length between inflection points as the span could be a possible alternative (Bakht and Jaeger, 1985) (Ebeido and Kennedy, 1996).
- Girder spacing is an important parameter (Zokaie et al, 1991) (Chen and Aswad, 1996) (Ebeido and Kennedy, 1996).
- Intermediate diaphragms do little good to improve the live load distribution. This is especially true in long bridges, where, ironically, they are most commonly used (Lin and Vanhorn, 1968) (Ebeido and Kennedy, 1996).

## CHAPTER 3 LIVE-LOAD TEST

A static load test was performed on the SR18/SR516 overcrossing, a three-span, slab on prestressed girder bridge. The truck used to apply loads was a 158 KN, (35.6 kip) two-axle, dump truck. Embedded vibrating-wire strain gages (VWSGs) were used to measure the response of the bridge. This chapter describes the bridge and the live-load test.

### 3.1 BRIDGE DESCRIPTION

Figure 3.1 shows a layout of the bridge and the girder designation system. Each of the five girder lines was denoted with a letter (A-E), and each span was identified with a number (1-3). At piers 1 and 4, the girders were supported on elastomeric bearings. At piers 2 and 3, grout pads were used.

Figure 3.2 shows a cross section of the bridge at Pier 2. The Washington State W74MG cross-section, shown in Figure 3.3, was used for all girders. Table 3.1 lists section properties of the girders. In the field, the girders were made composite with the 190-mm (7.5-in.) deck slab, which included a 10-mm (0.4-in.) integral-wearing surface. Field casting the pier diaphragms around reinforcement projecting from the girders made the girders continuous over Piers 2 and 3.

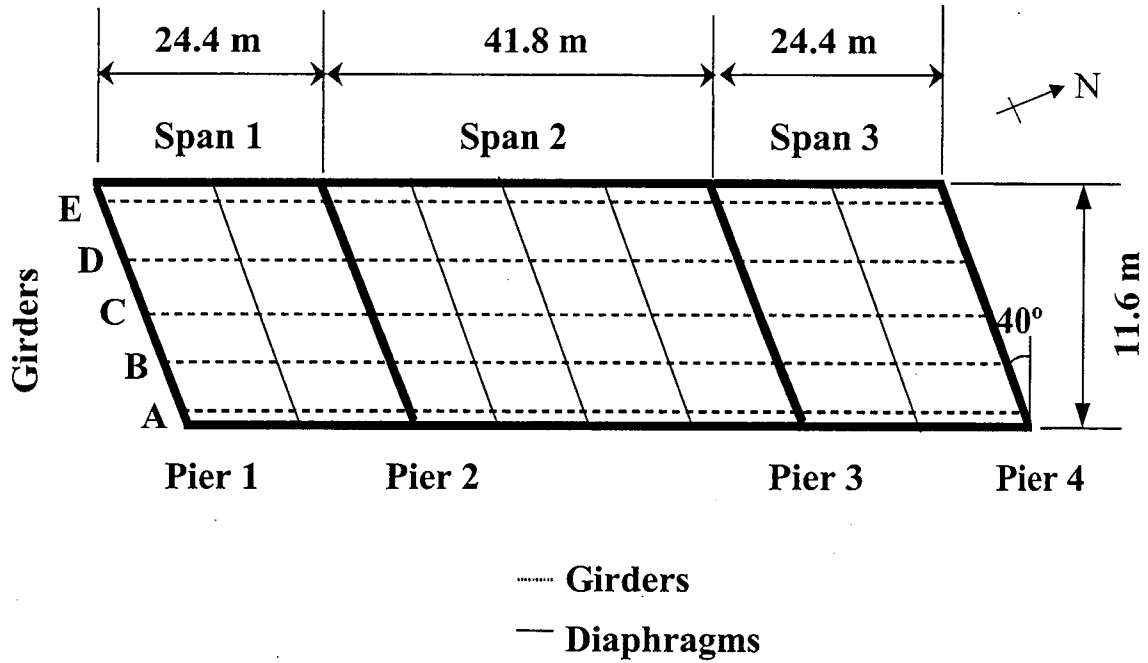


Figure 3.1. Bridge Layout

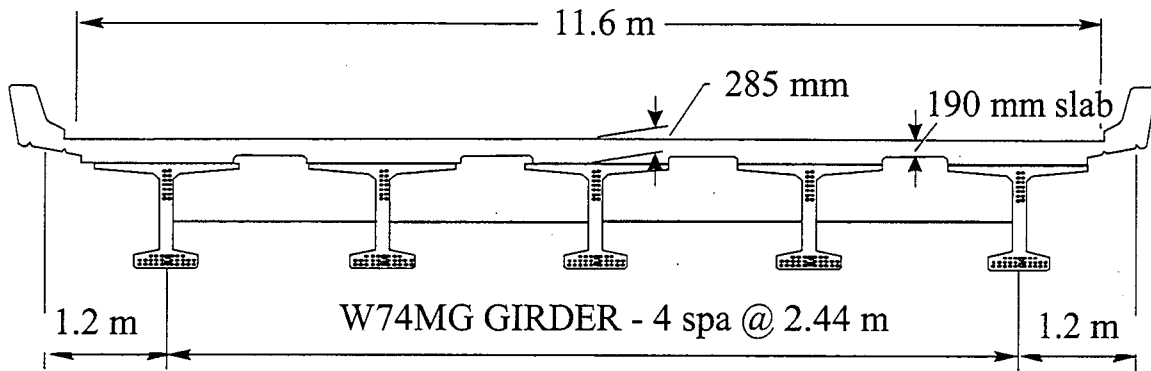


Figure 3.2. Bridge Cross-Section at Pier 2 (looking north)

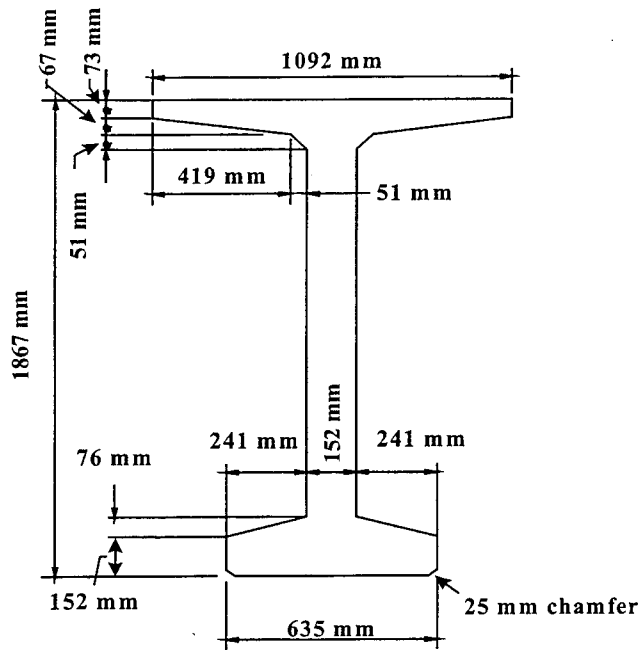


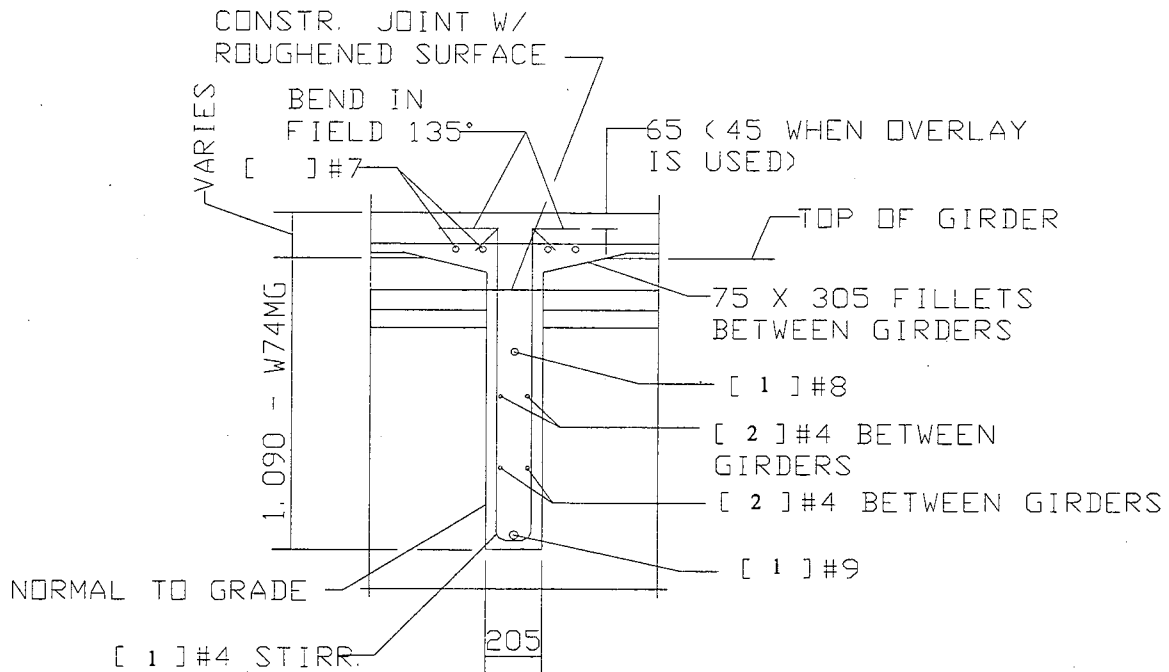
Figure 3.3. W74MG Girder Dimensions

Table 3.1. Section Properties

	Girder	Composite Section
Depth, mm	1 867	2 045
Area, mm <sup>2</sup>	485 300	765 100
I, mm <sup>4</sup>	227.5 x 10 <sup>9</sup>	400.4 x 10 <sup>9</sup>
y <sub>b</sub> , mm	970	1 330
S <sub>b</sub> , mm <sup>3</sup>	234.4 x 10 <sup>6</sup>	301.0 x 10 <sup>6</sup>
y <sub>t</sub> girder, mm	895	535
S <sub>t</sub> girder, mm <sup>3</sup>	254.3 x 10 <sup>6</sup>	748.8 x 10 <sup>6</sup>
y <sub>t</sub> slab, mm	-	715
S <sub>t</sub> slab, mm <sup>3</sup>	-	560.2 x 10 <sup>6</sup>

Intermediate diaphragms were placed at midspan for Spans 1 and 3, and at quarter spans along Span 2. The diaphragms were connected through the web of the girders with a #8 bar at the top of the diaphragms and a #9 bar at the bottom. The diaphragms were

cast on various days at the contractor's convenience. Figure 3.4 shows a typical intermediate diaphragm.



**Figure 3.4. Intermediate Diaphragms**

### 3.2 INSTRUMENTATION

Concrete strains were monitored with vibrating wire strain gauges (VWSGs) that were embedded in seven of the W74G bridge girders. These VWSGs monitored longitudinal strains in the girders as well as temperature. Because the number of gages installed in the girders was large, the fastest that the gages could be read reliably was at 3-minute intervals.

In the instrumented girders, gages were embedded both at 1.52 m (5 feet) from the end nearest Pier 2 and 457 mm (18 inches) from midspan towards Pier 2. Figure 3.5 shows plan and elevation views of the bridge, with the instrumentation sites marked. Each instrumentation site can be identified by span (1 or 2), girder (A, B, C, D or E) and span location (E or M).

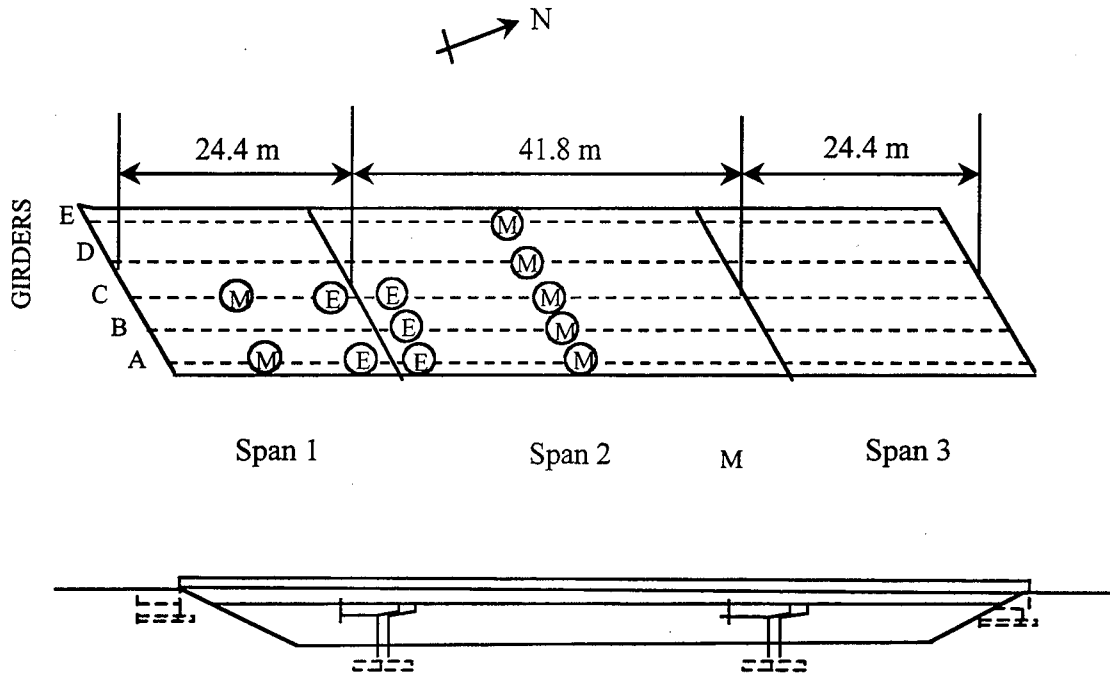


**Figure 3.5. Instrumentation Sites in HPC Bridge**

Girders A, B, and C were instrumented in the same manner (Figure 3.6). Two gages were placed in the bottom flange (BL and BR), three were placed in the web (LW, MW and UW) and one was placed in the top flange (TG). Girders D and E were instrumented only with bottom flange gauges (BL and BR).

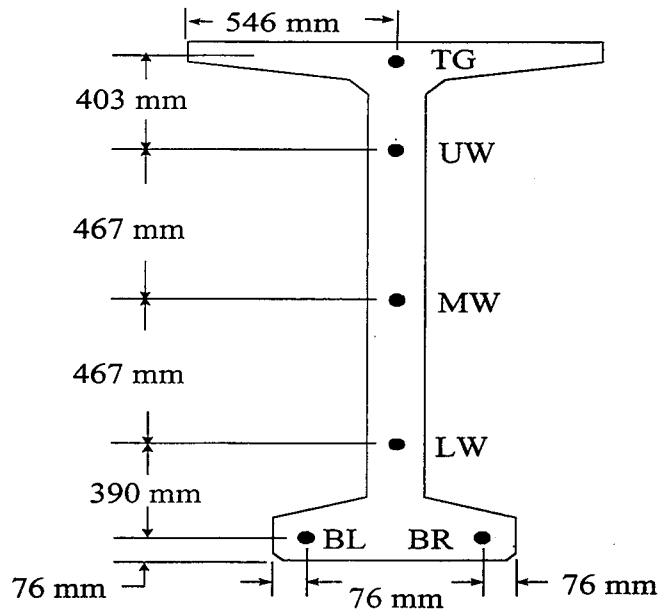


**Figure 3.6. Cross Section of Typical Instrumentation Site**

### 3.3 DESCRIPTION OF TRUCK

A single, two-axle dump truck that weighed 158 KN (35.6 kips) was used to apply loads to the bridge. Although the truck was not as large as an AASHTO design truck, it was the largest available at the time of the test. Figure 3.7 shows the truck's dimensions and axle loads.

### 3.4 TRUCK PLACEMENT

The center of gravity of the truck was placed at various locations in order to determine the bridge's response to live loads. For each girder line, the truck traveled from Span 1 to Span 3, stopping at each load location. Then it turned around and returned along the same line, stopping only at selected locations. The truck followed this same pattern for all five-girder lines.

Figure 3.8 shows a plan view of the bridge. At each single arrow location, a reading was taken with the truck facing in the direction of the arrow. Where two arrows point in opposite directions, a reading was taken with the truck facing each direction.

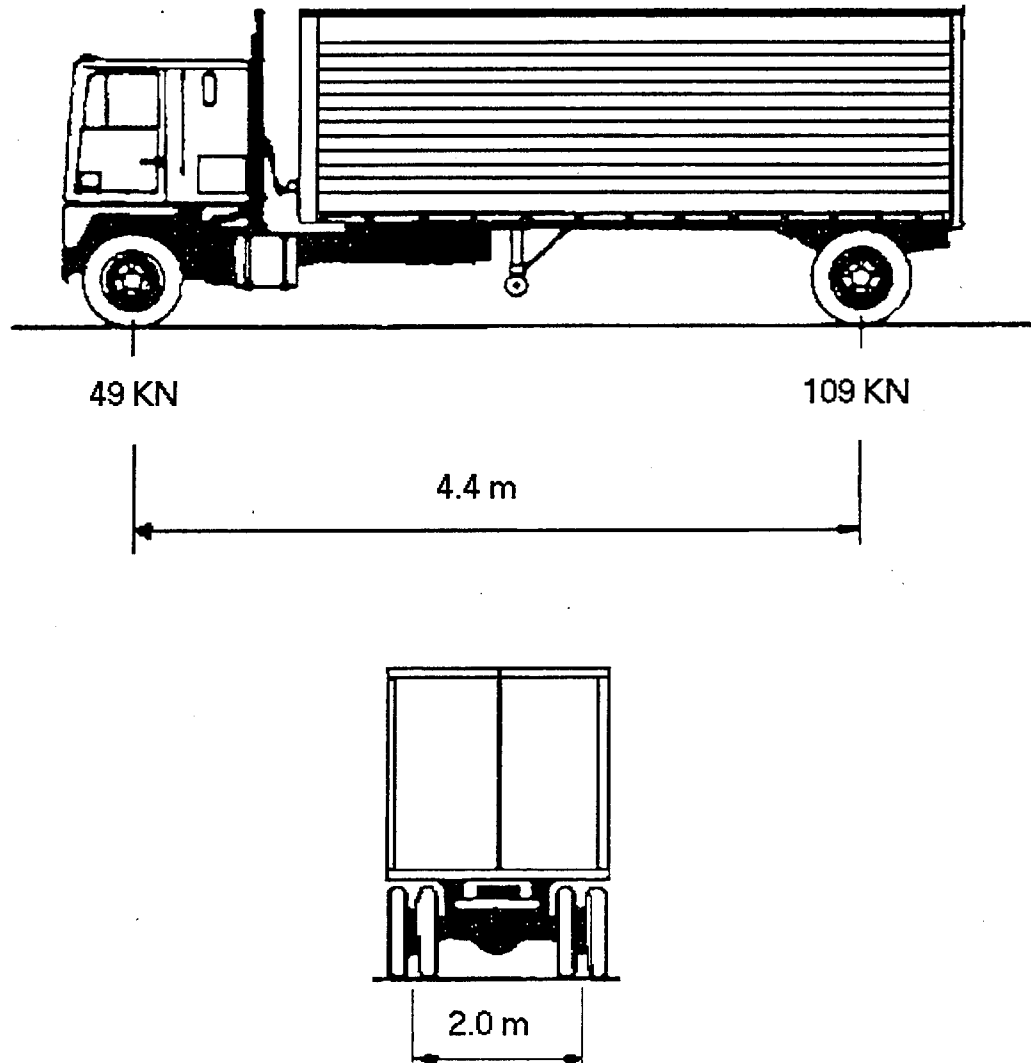


Figure 3.7. Truck Axle Loads and Dimensions

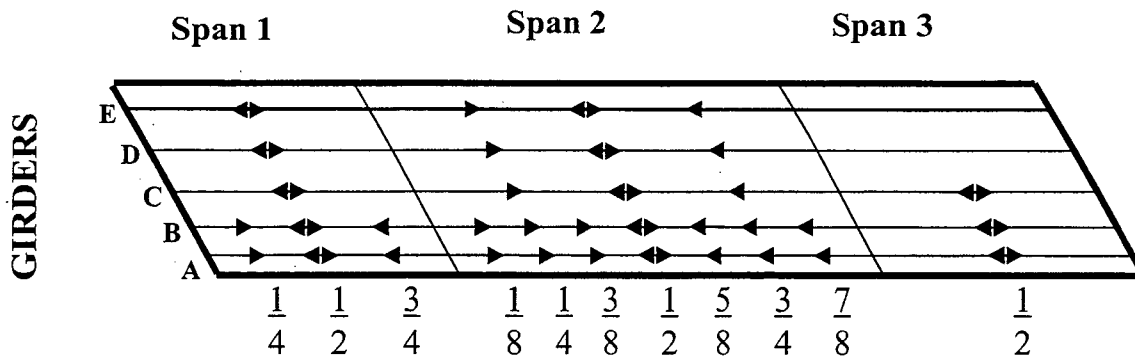


Figure 3.8. Truck Locations for Readings

## CHAPTER 4 FINITE ELEMENT MODELS

The SR18/SR516 bridge and a simply supported bridge (with a span equal to that of span 2) were modeled using a finite element program (SAP2000, 1997). Frame and shell elements were used to model the girders, deck, diaphragms, abutments and columns. The models were then used to evaluate response to truck and lane loading. This chapter describes the finite element models.

### 4.1 MODELING STRATEGY

Various finite element models of a simply supported beam were investigated to model the components of the bridge. Each model was compared with analytical solutions and with more complex models. When two models predicted the same result, the simpler model was chosen.

#### *4.1.1 Selection of Topology and Model Elements*

The modeling strategy was developed to evaluate the live load distribution procedures recommended by AASHTO, so it had to be sufficiently accurate to do so reliably. However its complexity had to be limited in order to run the analyses in a reasonable time and to express the output in ways that would be simple to handle. Therefore, considerable effort was put into selection of the overall topology and modeling of individual elements. Several constraints were recognized.

The first constraint was that the model had to be able to model truck loading of a variety of bridges with skew angles. This requirement dictated the need for a fine element mesh in the deck, so that nodes would be available near the truck wheels, regardless of the skew angle. A node spacing of 2 ft transversely, to fit the 8-ft girder

spacing, and 1 ft longitudinally was eventually chosen. This mesh had approximately 6000 nodes in the plane of the deck.

Many previous studies have shown that, in order to obtain accurate results, the flexural and torsional stiffnesses of the girders must be modeled correctly, and that the vertical placement of the members in the model must reflect that in the prototype. The most certain way to satisfy these requirements is to build all of the members such as girders and diaphragms, from a large number of solid brick elements. However, trials with structures simpler than the SR18/SR516 overcrossing showed that this procedure would lead to an unworkably large number of nodes and elements if the mesh in the cross-section was fine enough to reproduce the member properties adequately. After a number of trials, the arrangement of nodes and elements shown in Figure 4.1 was selected. It offered the following features:

- The deck, made from shell elements, contained enough nodes to permit satisfactory placement of the truck but consisted of only one layer of nodes.
- The vertical placement of the deck, lift and girder elements reflected accurately the locations of those members in the bridge. However, for convenience, the lift was modeled as if it had a constant depth of 95 mm (3.75 in.) although in reality, the depth varied over the span.
- The flexural and torsional properties of the precast girders could be lumped in the frame elements that were placed at the c.g. of the girders.
- Bending moments in the composite girders could be extracted from the output easily.
- The number of nodes was small enough (12,000) for a solution to be tractable.

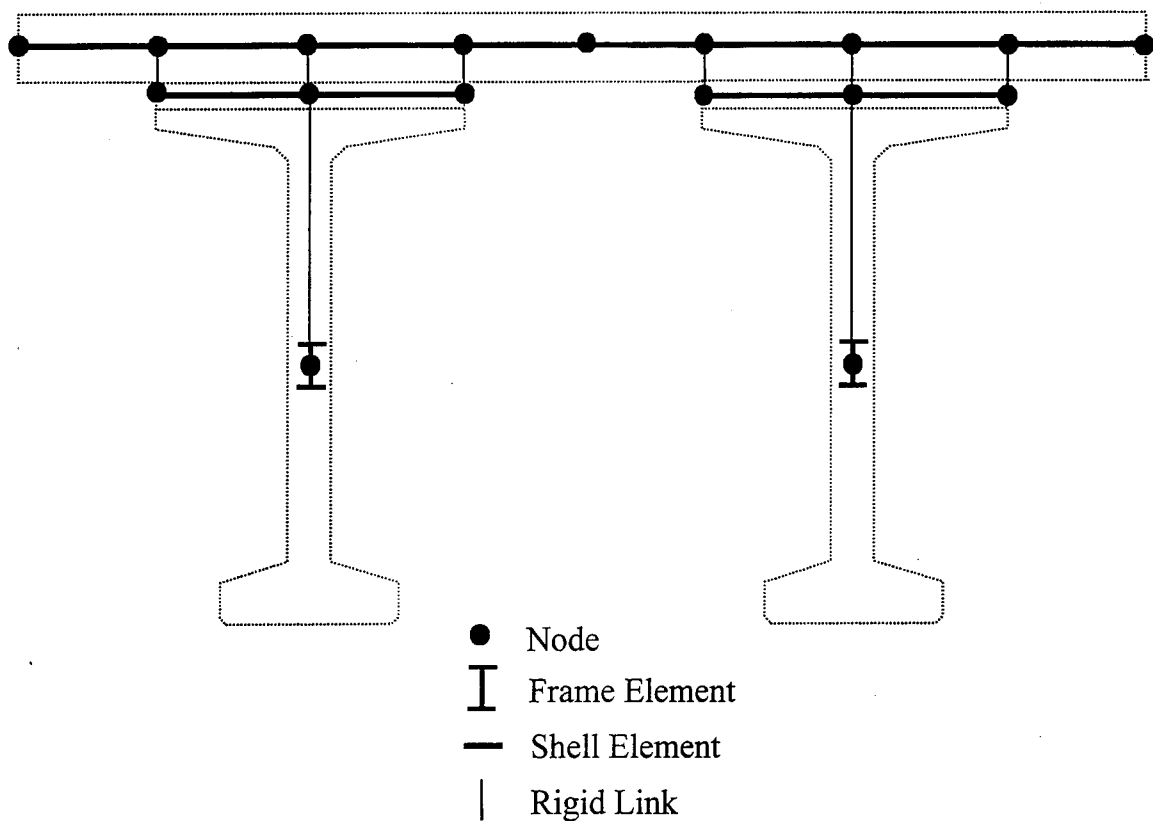


**Figure 4.1. Cross Section of Finite Element Model of Two Girders**

#### *4.1.2 Modeling of Girders*

The precast girders were represented by frame elements located below the deck. The most important girder properties to be reproduced in the frame elements were the axial, flexural and torsional stiffnesses. For the axial stiffness, only the element area had to be correct. The flexural stiffness of the frame element was set equal to that of the precast W74MG girder itself, and the correct composite action with the deck was assured

by attaching the frame element at the correct distance below the deck. The attachment required rigid links (constraint elements) that are discussed in Section 4.1.4.

The greatest change was modeling the torsional stiffness. First, no closed form method exists for finding the St. Venant torsion constant,  $J$ , of an irregular shape such as the W74MG. Second, the W74MG is an open section, so non-uniform, or restraint of warping, torsion plays a role in the response. It was necessary to determine whether its effects were significant in the SR18/SR516 bridge, because most computer programs, including SAP2000, have no provision for including it. It requires the addition of one degree of freedom per node and special elements.

These two issues were addressed simultaneously by identifying values for the St. Venant and restraint of warping torsion constants,  $J$  and  $C_w$ . Two finite element models were made of W74MG girders, using eight node solid bricks. Both were cantilevers, subjected to an applied torque at the free end. One was short (2.5 m (100 in.)) and one was long (25 m (1000 in.)). These lengths were selected on the basis of approximate analysis so that the short one would be dominated by restraint of warping torsion and the long one, by St. Venant torsion. The torsion equation and the closed form solution for the end twist angle in terms of  $J$  and  $C_w$  are shown in Equations 4.1 and 4.2.

$$M_T = GJ\phi' - EC_w\phi''' \quad (4.1)$$

$$\phi(X) = \frac{M_z}{GJ\lambda} [\lambda X - \sinh(\lambda X) + \tanh(\lambda l) [\cosh(\lambda X) - 1]] \quad (4.2)$$

where:  $M_T$  = applied torque

$$G = \text{shear modulus} = \frac{E}{2(1 + \nu)}$$

$J$  = Saint Venant torsional constant

$E$  = modulus of elasticity

$C_w$  = warping torsional constant

$\phi$  = angle of twist

$C_w$  and  $J$  were then identified by finding the values that gave the best fit between the finite element and closed form solutions. This was done by choosing  $C_w$ , then adjusting  $J$  so that the two solutions matched for the long cantilever (which was dominated by  $J$ ). Then that best estimate of  $J$  was used in the short cantilever to obtain an improved estimate of  $C_w$ . This iterative procedure was repeated until it converged, in this case after three cycles. The final values were  $J = 4.6 \times 10^9 \text{ mm}^4$  ( $11000 \text{ in}^4$ ) and  $C_w = 9.1 \times 10^{15} \text{ mm}^6$  ( $3.4 \times 10^7 \text{ in}^6$ ). Figure 4.2 shows the twist angle as a function of length for both the analytical and the finite element solutions for the long cantilever. They are nearly identical.

The need to include the warping torsion in the finite element model was then assessed by considering the twist angle at midspan of a W74MG girder subjected to a concentrated torque at mid span. (This test is somewhat too severe, because the loading is more concentrated than truck loading). The calculations were conducted using the closed form model. The difference in twist angle when warping torsion was or was not included was found to be only 0.15 percent. Furthermore, the characteristic length, given by

$$L_{ch} = \sqrt{EC_w/GJ} = 2.27 \text{ m (89 in.)}$$

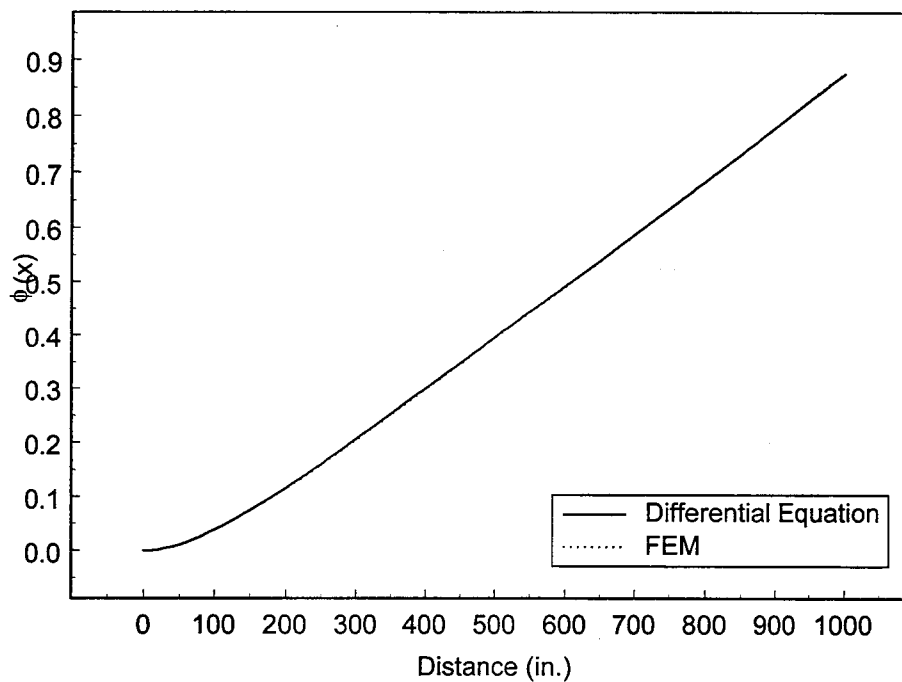


**Figure 4.2. Comparison of Differential Equation and FEM Solution**

is much smaller than the 41.8 m. (137 ft) length of Span 2, which indicates that the bridge response will barely be affected by restraint of warping. Restraint of warping was therefore ignored, and the frame element in Figure 4.1 was given only flexural, shear and St Venant torsion properties. The values are given in Table 4.1. The value of Young's modulus,  $E$ , for the girders was taken from cylinder tests, and Poisson's ratio,  $\nu$ , was assumed to be 0.20.

**Table 4.1. Properties for Girder Element**

Property	Girder
Area, mm <sup>2</sup> [in <sup>2</sup> ]	485300 [747.7]
J, mm <sup>4</sup> [in <sup>4</sup> ]	3.817 x 10 <sup>9</sup> [9170]
I <sub>x</sub> , mm <sup>4</sup> [in <sup>4</sup> ]	227.5 x 10 <sup>9</sup> [547400]
I <sub>y</sub> , mm <sup>4</sup> [in <sup>4</sup> ]	13.95 x 10 <sup>9</sup> [33500]
E, MPa [ksi]	34470 [5000]
$\nu$	0.2

#### ***4.1.3 Modeling of Deck, Girder Lift and Diaphragms***

The bridge deck, girder lifts and diaphragms were modeled using four-node shell elements. Eight nodel solid elements were also investigated, but the results were nearly identical to those from the shell elements, so the simpler shell elements were used. The properties for the deck, lifts and diaphragms are listed in Table 4.2. The value of the modulus of elasticity of the deck was taken from material tests on the deck. The modulus of elasticity of the diaphragms was assumed to be the same as that of the deck.

The intermediate diaphragms started 30.5 inches from the bottom of the girder and went to the bottom of the deck. The end and pier diaphragms were the full height of the girder. The pier diaphragms were made to act compositely with the pier caps through rigid constraints.

**Table 4.2. Deck, Lift and Diaphragm Properties**

Properties	Deck	Lift	Intermediate Diaphragms	Pier 2 & 3 Diaphragms	Piers 1 & 4 Diaphragms
Thickness, mm [in.]	190 [7.5]	95.3 [3.75]	203 [8]	1650 [65]	610 [24]
E, MPa [ksi]	31000 [4500]	31000 [4500]	31000 [4500]	31000 [4500]	31000 [4500]
$\nu$	0.2	0.2	0.2	0.2	0.2

The finite element model (Figure 4.1) is believed to reproduce nearly all the important structural features of the prototype. However, because the top flange of the precast W74MG girder is not modeled explicitly, its effect on the transverse deck stiffness is not included. This omission was deliberate because, in the prototype, the precast girders had cambered more than expected and so the lift near midspan was reduced to almost nothing. Because the nominal lift and the flange were almost the same thickness, the lower shell element in Figure 4.1 can be thought of as representing the girder flange instead of the lift. Modeling variations in lift thickness, both among girders and along the span, was considered impractical.

#### **4.1.4 Constraints**

Because the centroids of the girder, lift and deck elements did not coincide, they were connected by rigid-body constraints in order to ensure composite action. Rigid links were applied between the girder frame element, the lift shell elements and the deck shell element in the longitudinal direction to create composite action for major-axis bending. In the transverse direction, they connected the lift shell to the deck shell, in

order to ensure that the elements acted compositely and reproduced the correct transverse deck stiffness.

In addition to having the desired effect of creating a composite section, the constraints also imposed on the frame elements a zig-zag pattern of bending moments which overlay the true moment diagram, because the constraints inhibit nodal rotation. However, the effect of these spurious moments could be avoided by considering the moments at the mid-length of each one-foot long frame element.

#### 4.2 SR18/SR516 OVERCROSSING

The SR18/SR516 overcrossing superstructure, described in Chapter 3, was modeled using the techniques described in Section 4.1. In addition to the superstructure, that model included columns and a pier cap beam at the intermediate piers, and roller supports at each abutment. The columns were built up from 1-ft long frame elements, with the properties given in Table 4.3.

**Table 4.3. SR18/SR516 Column Properties**

Property	Column
Area (A), mm <sup>2</sup> [in <sup>2</sup> ]	46000 [1810]
Saint Venant Torsion (J), mm <sup>4</sup> [in <sup>4</sup> ]	217 x 10 <sup>9</sup> [521000]
Moment of Inertia about x and y axes (I <sub>x</sub> , I <sub>y</sub> ), mm <sup>4</sup> [in <sup>4</sup> ]	108 x 10 <sup>9</sup> [261000]
Modulus of Elasticity (E), MPa [ksi]	30300 [4400]
Length (L), mm [in.]	5590 [220]
Poisson's Ratio (ν)	0.2

### **4.3 SINGLE-SPAN BRIDGE**

To evaluate the effects of continuity, a finite element model of a single-span bridge with simple supports was also developed. It had the same geometry as Span 2 of the SR18/SR516 overcrossing, and was developed to provide an additional source of assessment of the AASHTO live load distribution factors. The end diaphragms in it resembled the Pier 1 diaphragms in the SR18/SR516 model.

### **4.4 VARIATIONS IN MODEL GEOMETRY**

The finite element (FEM) model of the SR18/SR516 overcrossing was first evaluated by comparing its predictions with the response measured during the field tests. This comparison is described in Chapter 5. Once the model had been validated, it was used to assess the live load distribution factors recommended in the AASHTO LRFD Specifications. This process is described in Chapter 6. Both the SR18/SR516 model and the single-span model were modified to create suites of bridge models that were similar to the basic ones but had different skews. The skew angles considered were 0°, 20°, 40°, 50° and 60°.

### **4.5 LOADING**

The weight of the dump truck was applied as four wheel loads on the deck with the centroid of the truck at the load site (Figure 3.8). Because the locations of the wheel loads did not coincide with nodal locations, simple shape functions were used to distribute the wheel loads to the four nodes of the shell elements. Equations 4.3 to 4.6 list the shape functions. In these equations, the wheel is located at  $(x, y)$ . Figure 4.3 shows the notation used for the symbols in the shape functions.

$$N_1 = \frac{1}{4ab}(a-x)(b-y) \quad (4.3)$$

$$N_2 = \frac{1}{4ab}(a+x)(b-y) \quad (4.4)$$

$$N_3 = \frac{1}{4ab}(a+x)(b+y) \quad (4.5)$$

$$N_4 = \frac{1}{4ab}(a-x)(b+y) \quad (4.6)$$

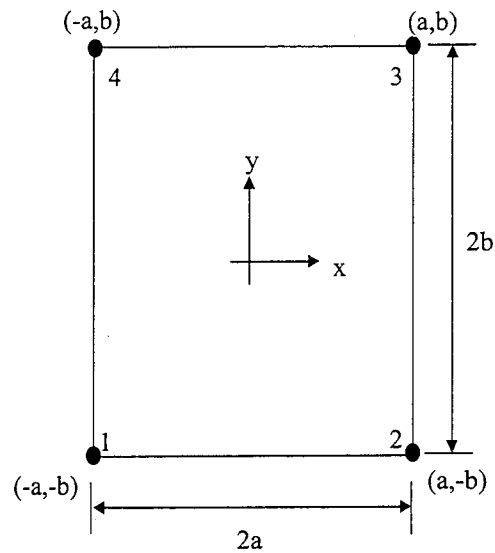


Figure 4.3. Notation for Shape Function Definition

#### 4.6 CALCULATED MOMENTS

The finite element output included axial forces and moments for the frame elements (W74MG girder), and top and bottom stresses for the shell elements (lift and deck). The composite cross-sectional moments were found by calculating the stress at the bottom of the girder due to the axial force and moment from the frame element

(Equation 4.7) and then multiplying this stress by the theoretical composite section modulus (Equation 4.8).

$$f_g = P/A + M_g/S_g \quad (4.7)$$

$$M_c = S_{gc} f_g \quad (4.8)$$

where:  $f_g$  = stress at bottom flange of girder

$P$  = axial force in frame element

$A$  = cross-sectional area of girder

$M_g$  = moment in frame element

$S_g$  = bottom section modulus of girder

$M_c$  = composite cross-sectional moment

$S_{gc}$  = bottom composite section modulus

## CHAPTER 5 EVALUATION OF ANALYTICAL MODEL

Loads with the same magnitude and pattern as the dump truck were applied to the finite element model (Chapter 4) at some of the same locations that the truck had been placed on the bridge (Section 3.4). The moment computed by the finite element model was compared with the moment calculated from the measured strain readings to verify that the model accurately predicted the bridge's response. Chapter 5 describes this evaluation.

### 5.1 MEASURED MOMENT

The composite cross-sectional moments were calculated from differences in strain readings between the loaded and unloaded bridge. Prior to placing the truck at reading locations along a girder line, initial strain and temperature readings were taken with the truck off the bridge. After the strain readings were measured for a particular girder line, a second zero reading was taken. Any change in zero readings was assumed to be a result of thermal effects. Individual zero readings for every load location was found by linearly interpolating on temperature (based on the gage temperature at the time of loading) between the initial and final zero reading. The change in strain, due to the application of the dump truck, was calculated by subtracting the measured strain when the truck was at the load location from the interpolated zero reading. The composite cross-sectional moment was calculated using Equation 5.1.

$$\Delta M_c = \frac{E * \Delta \epsilon * I}{C} \quad (5.1)$$

where:  $\Delta M_c$  = change in composite cross-sectional moment due to live load

$E$  = modulus of elasticity (34000 MPa (5000 ksi))

$\Delta \varepsilon$  = measured change in strain

$I$  = composite moment of inertia ( $5.41 \times 10^{10}$  mm<sup>4</sup> (1260000 in<sup>4</sup>))

$C$  = distance from composite centroid to gauge location (1510 mm (59.6 in.))

## 5.2 MIDSPAN LOADING

During the field testing, the centroid of the truck was placed at midspan of each girder in span 2 (Figure 3.8). The response of the finite element model of the SR18/SR516 overcrossing was analyzed for this same loading condition. The FEM midspan response to each girder was then compared with the measured response from the VWSGs for each of the girders except girder D, which did not have a functioning VWSG. Figure 5.1 compares the FEM and measured moments for all five girders when the truck is placed on girders A and B.

For girders A and B, the measured moment was calculated from the average strain reading in the bottom of the girder (gauges BL and BR). In the case of girders C and E, only one of the bottom gauges in each of the girders was functioning at the time of the live load test, so the moment was calculated from only one gauge. As expected, the moment was largest in the girder over which the truck was placed and diminished progressively in the more distant girders.

The maximum moment for girders A, C and E occurred when the truck was placed directly over the girder in question. The largest moment in B occurred when the truck was placed directly over girder A. Although girder D did not have a functioning

VWSG, the FEM output indicates that the largest moment for girder D occurred when the load is placed on girder E.

The SR18/SR516 overcrossing behaved as if it were continuous. However, the continuity might change in the future due to continued cambering of the girders or the addition of daily traffic on the bridge. The continued cambering of the girders would cause bottom cracks at the intermediate piers and would therefore reduce the continuity. Because the deck casting occurred nearly 7 months after the girders were initially cast (Barr et al., 1998), it is not likely that continued cambering of the girders would eliminate the continuity. However, the addition of daily traffic may reduce the degree of continuity of the bridge.

Figure 5.2 shows a comparison between calculated and measured moments at midspan due to placement of a single truck at midspan. Five load cases, each represented by a different symbol, are included. Each load case consists of a truck placed over a girder, and has four associated response locations (girders A, B, C, E). The abscissa is the moment derived from the strain gauge measurements, and the ordinate is the moment that was calculated from the FEM model. The straight line represents a perfect correlation between the FEM moment and the measured moment.

In general, the moment from the finite element model was similar to the moment calculated using the measured data. The FEM moment was a little larger in almost all cases but was within 6% of the moment predicted from the SR18/SR516 FEM model for the moment directly under the load. The average difference was 16.8 kN-m (149 kip-in.), which corresponds to 1.4 microstrain. Some scatter in the measured data must be

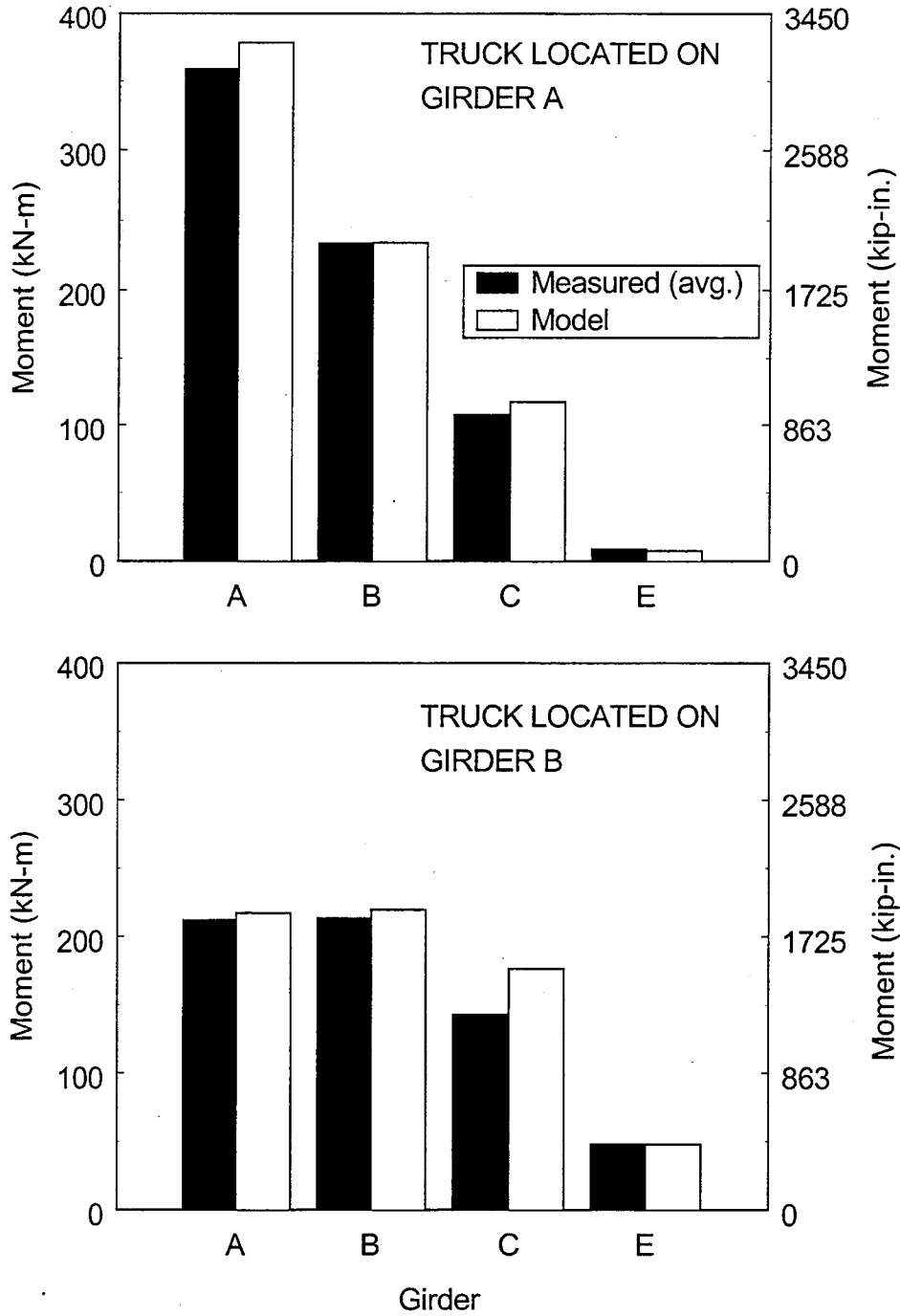


**Figure 5.1. Midspan Response Due to Midspan Loading**

expected because, despite the considerable weight of the truck, the largest measured strain was only 32 microstrain. This value was obtained by the procedures described in Section 5.1. Despite efforts to remove all thermal effects, some residual error is inevitable.

The circle and inverted triangle in the top right corner of Figure 5.2 are the response of the exterior girders due to a load on the midspan of the respective exterior girder. These responses are much larger than the responses of the other girders.

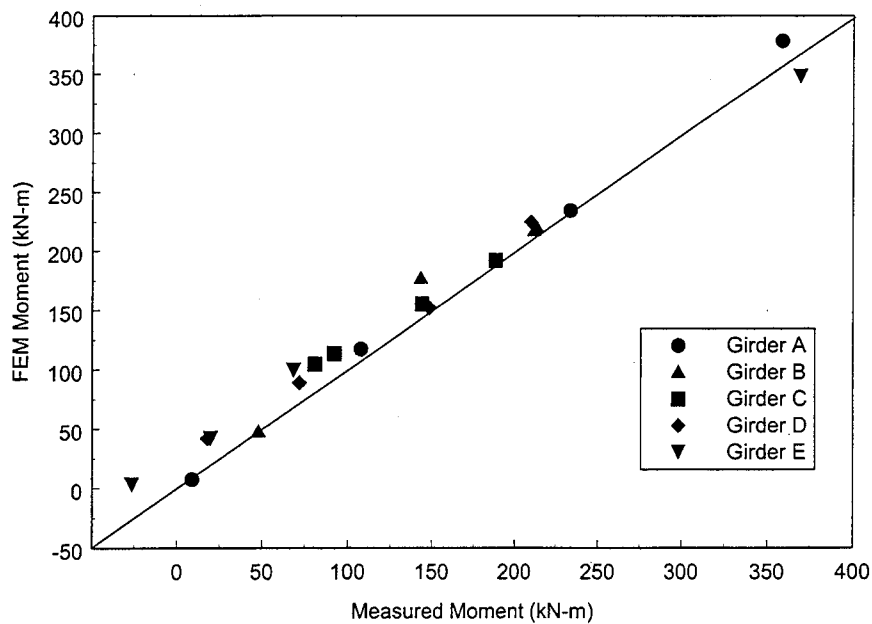


Figure 5.2. Comparison of Midspan Moment from FEM Model and VWSGs

### **5.3 INFLUENCE LINE**

The midspan moments from the FEM and the strain measurements were also compared as the truck was placed at various locations along the length of a girder. This comparison allowed the model to be evaluated due to loads at locations other than midspan. Figure 5.3 shows the influence lines for midspan moment in Span 2 for girders A and B. FEM results and data from the average bottom strains gauges are shown. For the FEM, loads were placed at quarter points in Spans 1 and 3 and at eighth points in Span 2. For the measured moments, loads were placed at the locations shown in Figure 3.8.

For both girder lines the FEM moments and the VWSG moments had identical trends and were numerically similar. In girder line A, the measured moment was smaller than the FEM moment when the truck was in Span 1, but was similar when the truck was in Spans 2 and 3. Both measured and predicted moments were similar throughout girder line B.

### **5.4 FINITE ELEMENT MODEL: SUMMARY AND CONCLUSION**

A finite element model of the SR18/SR516 overcrossing was developed. It consisted of frame elements, shell elements and rigid link (constraint elements). Particular attention was paid to ensure that the elements were placed in the correct vertical locations and that the torsional properties of the girders were correctly simulated. The model included columns, piercaps, lifts, end diaphragms and intermediate diaphragms.

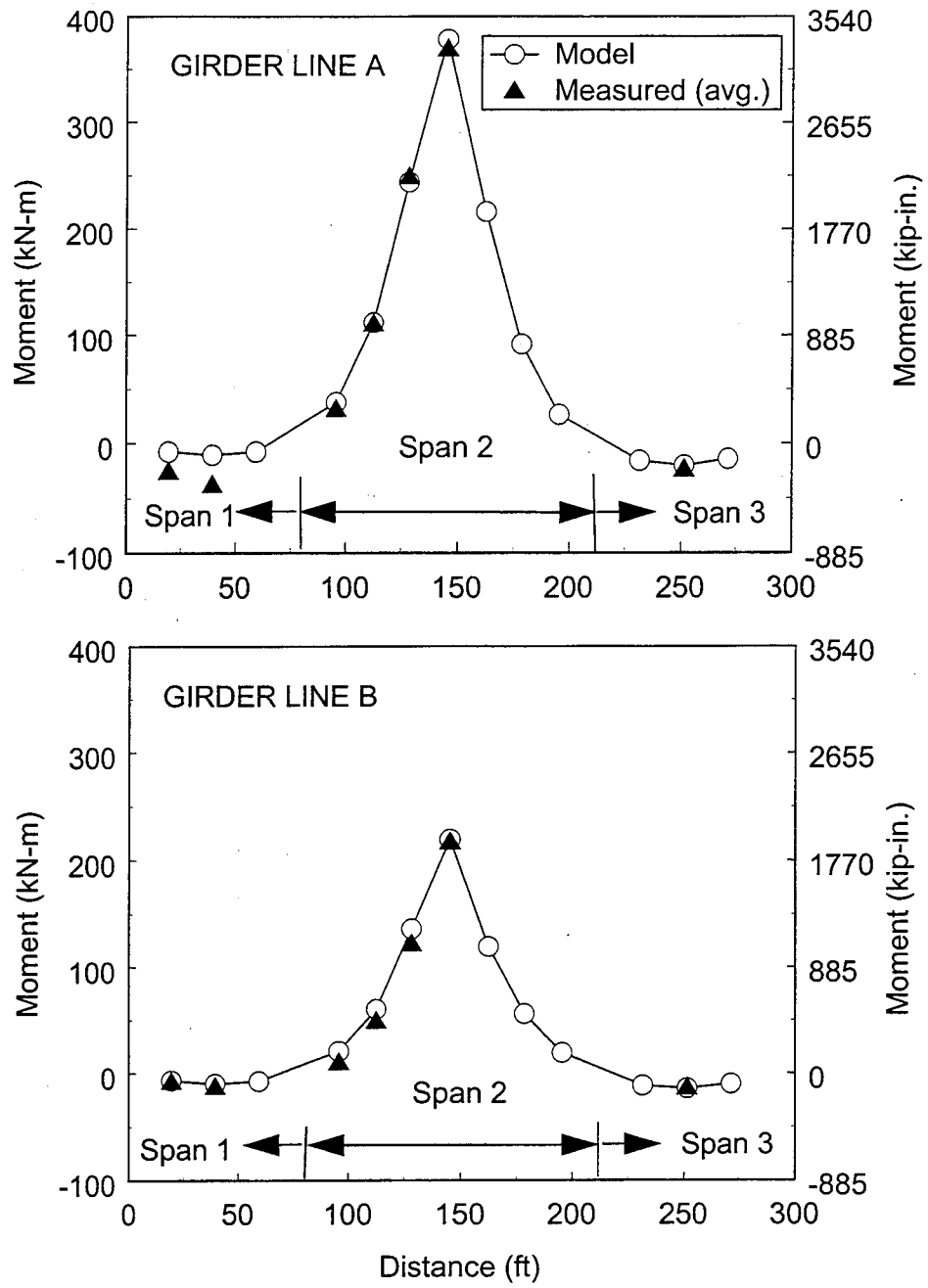


Figure 5.3. Influence Lines for Midspan Moment

The model was loaded with point loads that simulated a dump truck that was used to conduct a field load test. The truck was placed in many locations. The results predicted by the finite element model were compared with those computed from the strains measured during the field test. The correlation was close, despite the small measured strains and the difficulties of maintaining experimental accuracy under these conditions.

The close correlation was taken as a validation of the accuracy of the finite element model.

## **CHAPTER 6**

### **LIVE LOAD DISTRIBUTION FACTORS**

Chapter 6 describes an evaluation of the live load distribution factors for the SR18/SR516 overcrossing. These factors were computed with finite element analysis (FEA). These factors are then compared with distribution factors obtained from the methods in three codes (AASHTO LRFD Specification, AASHTO Standard Specifications and the Ontario Highway Bridge Design Code (OHBDC)).

The influence of lifts, intermediate diaphragms, end diaphragms and continuity on the live load distribution factors is also investigated.

#### **6.1 CODE LIVE LOAD DISTRIBUTION FACTORS**

The use of live load distribution factors allows a designer to analyze bridge response by treating the longitudinal and transverse effects of wheel loads as uncoupled phenomena. Many codes have adopted simple procedures for calculating live load distribution factors for bridges in order to simplify the girder design procedure. The designer computes the girder design moment by applying a prescribed load to a single girder and then multiplying the resulting maximum girder moment by the live load distribution factor. The design moment is intended to represent the maximum moment in the girder when all possible truck combinations and locations are considered. Bridge design codes contain simple equations or charts for computing approximately the live load distribution factors. These methods requires much less design effort than would multiple finite element analyses, but, as is shown in this chapter, their results can differ significantly.

Because the various code calculation methods produce different results, bounds on the values of the live load distribution factors are worth considering. For a bridge with zero skew, the lowest possible value of the live load distribution is  $N_L/N_G$  times the multiple lane reduction factor, where  $N_L$  = number of lanes,  $N_G$  = number of girders. This minimal value occurs when the load is equally shared among all girders. In the case of the SR18/SR516 overcrossing, this value is  $3/5*0.85 = 0.51$ , if 3-lane loading controls and  $2/5*1.0=0.40$  if 2-lane loading controls.

The methods used to calculate the live load distribution factors that were investigated in this study were those given in the AASHTO LRFD Specification (1994), AASHTO Standard Specification (1996) and the Ontario Highway Bridge Design Code (OHBDC) (1992).

#### ***6.1.1 AASHTO LRFD Specification Factors***

Of the codes investigated, the AASHTO LRFD Specifications (1994) is the most recently adopted so it would be expected to give the best results. The maximum moment due to an AASHTO design truck is first calculated by placing the truck in various locations along the girder. The design moment for the girder is then found by multiplying the maximum moment by the live load distribution factor.

The distribution factor for an interior girder used in a concrete bridge with two or more lanes is calculated using Equation 6.1. Another equation is given for a bridge with only one design lane. These two equations implicitly contain a multi-lane reduction factor.

$$DF = 0.075 + \left(\frac{S}{9.5}\right)^{0.6} \left(\frac{S}{L}\right)^{0.2} \left(\frac{K_g}{12.0Lt_s^3}\right)^{0.1} \quad (6.1)$$

where:  $DF$  = Distribution Factor for interior girder

$S$  = girder spacing (ft)

$L$  = span length (ft)

$K_g$  = longitudinal stiffness parameter (in<sup>4</sup>)

$$= n(I + Ae_g^2)$$

$n$  = modular ratio between girder and deck material

$I$  = moment of inertia of girder (in<sup>4</sup>)

$A$  = area of girder (in<sup>2</sup>)

$e_g$  = distance between the center of gravity of basic girder and deck (in.)

$t_s$  = thickness of deck

The distribution factor for an exterior girder is calculated by applying a correction factor to the distribution factor for an interior girder (Equation 6.1). This correction is either applied using Equation 6.2 or a pile reaction analysis. In the case of the SR18/SR516 overcrossing, Equation 6.2 controlled the design.

$$e = 0.77 + \frac{d_e}{9.1} \geq 1.0 \quad (6.2)$$

where:  $e$  = exterior girder correction factor

$d_e$  = distance between the center of exterior beam and the interior edge of curb or traffic barrier (ft)

The AASHTO LRFD code also takes into account the effect of skew on the distribution factors. This modification is accomplished by multiplying the distribution

factors for both the interior (Equation 6.1) and exterior girders (Equations 6.1 and 6.2) by a skew correction factor (Equation 6.3).

$$sk = 1 - c_1(\tan\theta)^{1.5} \quad (6.3)$$

where:  $sk$  = skew correction factor

$$c_1 = 0.25 \left( \frac{K_g}{12.0L_t^3} \right)^{0.25} \left( \frac{S}{L} \right)^{0.5}$$

if  $\theta < 30^\circ$  then  $c_1 = 0.0$

if  $\theta > 60^\circ$  use  $\theta = 60^\circ$

### **6.1.2 AASHTO Standard Specification Factors**

The method for calculating girder design moment presented in the AASHTO Standard Specification (1996) is the simplest of the three investigated. The AASHTO Standard Specification and AASHTO LRFD use the same procedure for finding the maximum moment due to an AASHTO truck, except that only half of each axle load is used in the Standard Specification. The girder design moment is found by multiplying the maximum moment by the distribution factor calculated with Equation 6.4.

$$DF = \frac{S}{5.5} \quad (6.4)$$

The AASHTO Standard Specification does not distinguish between exterior and interior girders, nor does it provide any correction for the effect of skew. It requires the use of a multilane reduction factor of 0.9 for 3-lane bridges. This factor was applied to the Standard Specification distribution factors when comparing them with the results of

the finite element distribution factors in this study. Also, because the Standard Specification only uses half of the AASHTO axle loads, the distribution factors predicted by the Standard Specification were divided by two in order to compare them directly with the LRFD and finite element distribution factors.

### 6.1.3 OHBDC Factors

The OHBDC's (1992) method for calculating the live load distribution factor is based on orthotropic plate behavior. The maximum static girder moment is found by applying to an isolated girder one line of wheel loads from the OHBDC truck or one-half of a lane load. The maximum moment is then multiplied by the OHBDC distribution factor to obtain the girder design moment.

The distribution factors predicted by the OHBDC are computed using the various stiffnesses of the bridge components. Dimensionless stiffness ratios are first calculated using Equations 6.5 and 6.6.

$$\alpha = \frac{D_{xy} + D_{yx} + D_1 + D_2}{2(D_x D_y)^{0.5}} \quad (6.5)$$

$$\theta = \frac{b}{L} \left[ \frac{D_x}{D_y} \right]^{0.25} \quad (6.6)$$

where:       $\alpha$  = torsional parameter  
 $D_x$  = longitudinal flexural rigidity per unit width  
 $D_y$  = transverse flexural rigidity per unit length  
 $D_{xy}$  = longitudinal torsional rigidity per unit width

$D_{yx}$  = transverse torsional rigidity per unit width

$D_1$  = coupling rigidity per unit width

= v (lesser of  $D_x$  and  $D_y$ )

$D_2$  = coupling rigidity per unit width

=  $D_1$

$b$  = half-width of bridge

$L$  = span of bridge

After  $\alpha$  and  $\theta$  are calculated, the initial load distribution factor,  $D$ , for interior and exterior girders is found from two design charts. A correction factor,  $C_f$ , is also obtained from a design chart. The load distribution factor,  $D_d$ , which is applied to the maximum static moment is calculated using Equation 6.7. Figure 6.1 is a copy of the OHBDC's three-lane bridge chart for the initial load distribution factor.

$$D_d = D \left[ 1 + \frac{\mu C_f}{100} \right] \quad (6.7)$$

where:  $D$  = initial load distribution factors (from design charts)

$$\mu = \frac{W_e - 3.3}{0.6}$$

$W_e$  = width of design lane in meters

$C_f$  = correction factor

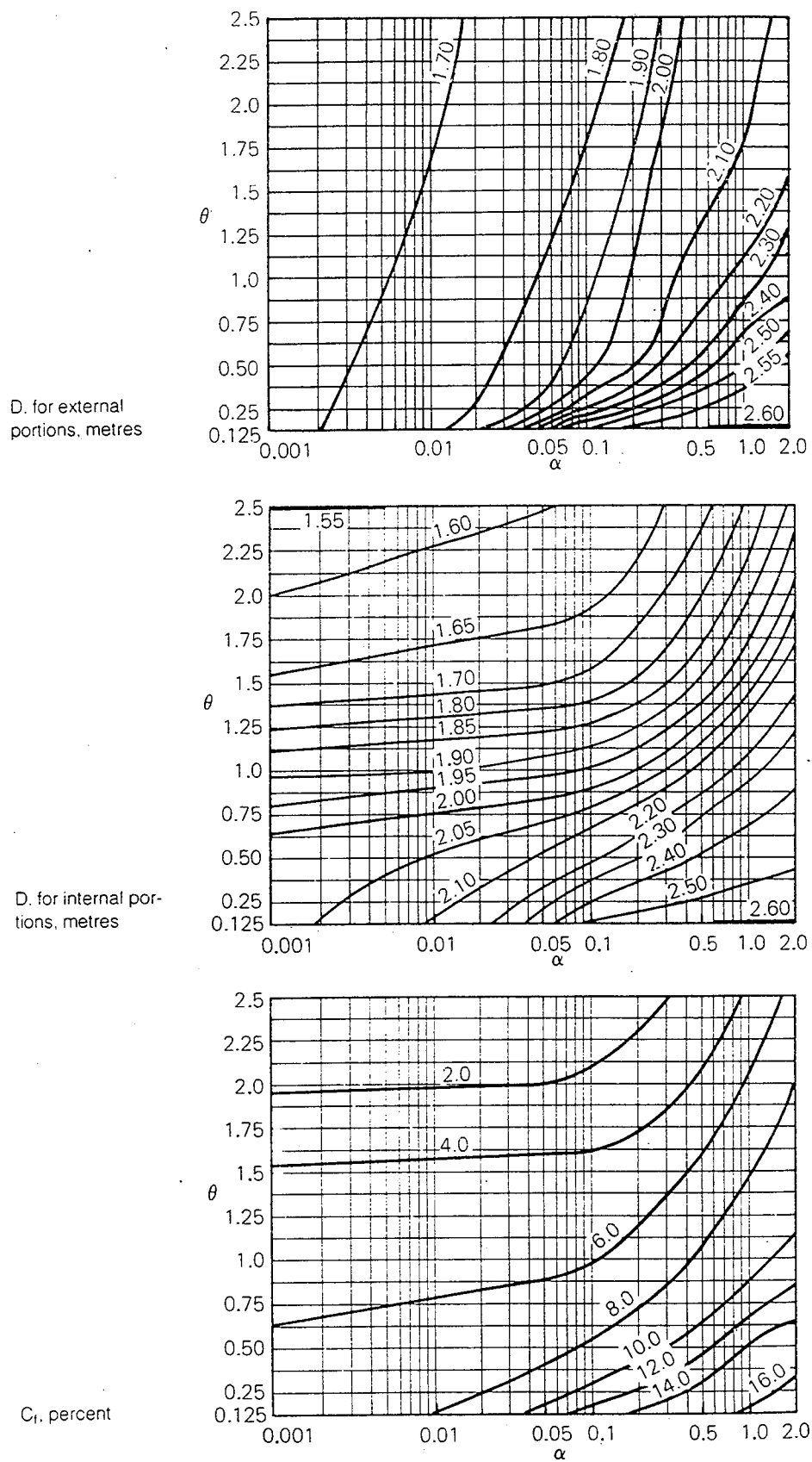


Figure 6.1. OHBDC Three-Lane Bridge Live Load Distribution Coefficient Chart

The OHBDC load distribution factors are only valid for skew angles up to 20 degrees. In addition, the initial load distribution factor ( $D$ ) already includes a multilane reduction factor. As with the Standard Specification, the OHBDC only uses half of the truck axle load. Therefore the distribution factors predicted by the OHBDC were divided by two in order to compare them directly with the LRFD and finite element distribution factors.

## 6.2 FINITE ELEMENT MODELS

Five progressively more detailed models of the SR18/SR516 overcrossing were developed using the finite element program SAP2000 (SAP2000, 1997). They were:

- Model 1 - a single span model of Span 2 with only the deck and girders modeled (no lifts, diaphragms or span continuity)
- Model 2 – same as Model 1, but lifts were modeled between the girders and deck
- Model 3 – same as Model 2, but intermediate diaphragms were added
- Model 4 – same as Model 3, but end diaphragms were added
- Model 5 – same as Model 4, but Spans 1 and 3 were added, and the three spans were made continuous. This model best represents the SR18/SR516 overcrossing

The purpose of developing the five models was to study the influence that the lifts, intermediate diaphragms, end diaphragms and continuity had on the live load distribution factors. By adding one member type at a time, its influence on the distribution factors could be isolated. To evaluate the effect of skew the skew angle of each model was varied between 0 and 60 degrees.

The material properties used in each model were derived from material tests on concrete from the SR18/SR516 overcrossing. For Span 2 models with intermediate diaphragms (Models 3 and 4), diaphragms were located at the quarter points. The SR18/SR516 model (Model 5) had intermediate diaphragms at midspan in Spans 1 and 3 and at quarter points along Span 2. In Model 5, thick pier diaphragms that were considerably torsionally stiff were located at the intermediate supports.

### 6.3 LOADING SCHEME

The live load distribution factors are intended to represent the envelope of all possible load cases, so many loading configurations were investigated using the AASHTO standard truck and the AASHTO uniform lane loading. In all cases, only the midspan moment was considered. Because the bridge is wide enough to accommodate three lanes, both two and three lane-loading conditions were considered, even though the bridge only contains two traffic lanes in its present configuration. For all loading conditions, the midspan moment was calculated in each of the five girders.

For each model, the longitudinal position of the AASHTO trucks was established by finding the location where an AASHTO truck produced the maximum midspan moment on an isolated beam of the same span. The AASHTO trucks were then placed longitudinally in the same position on the finite element model.

The transverse locations of the AASHTO trucks were found by dividing the bridge into as many 12-ft wide lanes as possible (3) and then systematically moving individual trucks within their respective lane (35 load cases). Lanes were also systematically moved in order to simulate many transverse-loading conditions (Zodaie et

al., 1991). In developing the load cases, it was assumed that the center of the wheels could be placed no closer than 0.61 m (2 ft) to the edge of the barrier. Figure 6.2 shows the loading configuration that controlled for the exterior girders.

In a second series of load cases, an AASHTO distributed lane load of 9.3 kN/m (0.64 kip/ft) was applied to the lanes of each model. This lane load was moved within each lane over a 3.0-m (10-ft) width and nine load cases were analyzed. The load was applied as point loads at the nodes and was assumed to simulate a uniform load because the mesh spacing was small compared with the span.

In each model and load case, the midspan moments in each girder were recorded. The moments were subsequently used as the basis for comparison of the live load distribution factors.

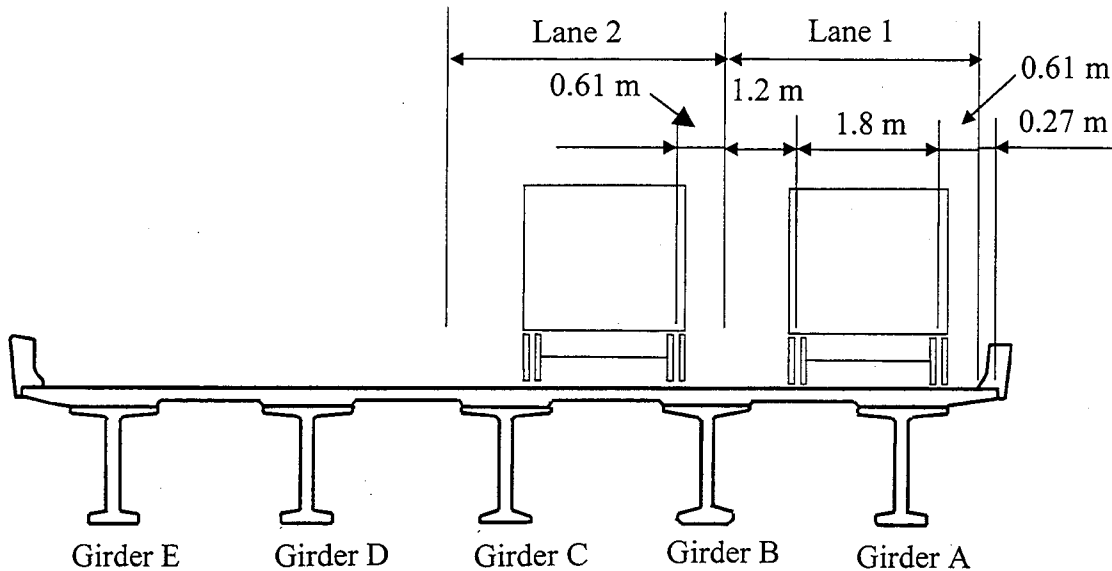


Figure 6.2. Example Loading Scheme for Two-Lane Loading

## 6.4 EVALUATION OF CODE LIVE LOAD DISTRIBUTION FACTORS— TRUCK LOADING

The moments derived from the finite element models (Section 6.3) were used to calculate the distribution factors as follows. First, a multilane reduction factor of 0.85 was applied to all the moments calculated with a three-lane load condition, and a factor of 1.0 was applied to all the moments calculated with the two-lane load condition. After application of the multilane loading factor, the maximum moment was obtained for each of the five bridge girders. Third, the maximum exterior and interior moments were obtained. Finally, the distribution factors for the interior and exterior girders were found by dividing the maximum factor moment by the static moment found when the AASHTO truck was placed on the isolated beam (Section 6.3). In all cases, the finite element model results were computed for skew angles ranging from 0° to 60°.

The results from the finite element models were compared with the live load distribution factors taken from three codes:

- AASHTO LRFD Specification (1994)
- AASHTO Standard Specification (1996)
- Ontario Highway Bridge Design Code (OHBDC) (1992)

Section 6.4.1 compares the distribution factors obtained from Models 1 and 5 with those obtained from the codes. Section 6.4.2 illustrates the effects of adding lifts to the finite element model by comparing Models 1 and 2. Section 6.4.3 shows the effects of adding intermediate diaphragms by comparing Models 2 and 3. The effects of adding end diaphragms are shown in Section 6.4.4 by comparing Models 3 and 4. Section 6.4.5

shows the effect of adding side spans and making the bridge continuous, by comparing Models 4 and 5.

#### ***6.4.1 Comparison of Code Factors with Those Derived from FEA***

Figure 6.3 shows the distribution factors from the three codes and finite element Models 1 and 5. Separate plots are provided for exterior and interior girders. The distribution factors are plotted for skew angles ranging from 0 to 60 degrees. The code distribution factors are shown with open symbols, and those from the finite element models are shown with solid symbols. The OHBDC distribution factors are only valid for bridges with skew angles less than 20 degrees and are therefore only plotted up to 20 degrees. The following conclusions are apparent from Figure 6.3.

- Model 1 is probably the best basis for comparison with the AASHTO LRFD, because the research on which it was based used a similar single-span model. Model 5 is the most representative of the SR18/SR516 overcrossing.
- The AASHTO LRFD live load distribution factors follows the same trend as the FEA in that they diminish with increasing skew. The average difference between the distribution factors from the LRFD code and those from Model 1 was 6 percent. This is close to the 5 percent reported by Zokaie (1991). The difference between the distribution factors from Model 5 and the LRFD code ranged from 24 percent (exterior girder, 0° skew) to 35 percent (exterior girder, 60° skew) lower.
- The AASHTO Standard Specification does not account for skew, while the other codes do. Model 1 predicts distribution factors that are closer to those that are given in the Standard Specification than Model 5. The difference between the

distribution factors from FEA and the Standard Specification ranged from 4 percent unconservative (Model 1, 0° skew, exterior) to almost 43 percent conservative (Model 5, 60° skew, interior).

- In contrast to the findings of Mabsout et al. (1997), the AASHTO LRFD distribution factors were found to be more conservative than those of the Standard Specifications at low skew angles.
- The OHBDC predictions are very close to those of Model 5 for skew angles less than 20°.

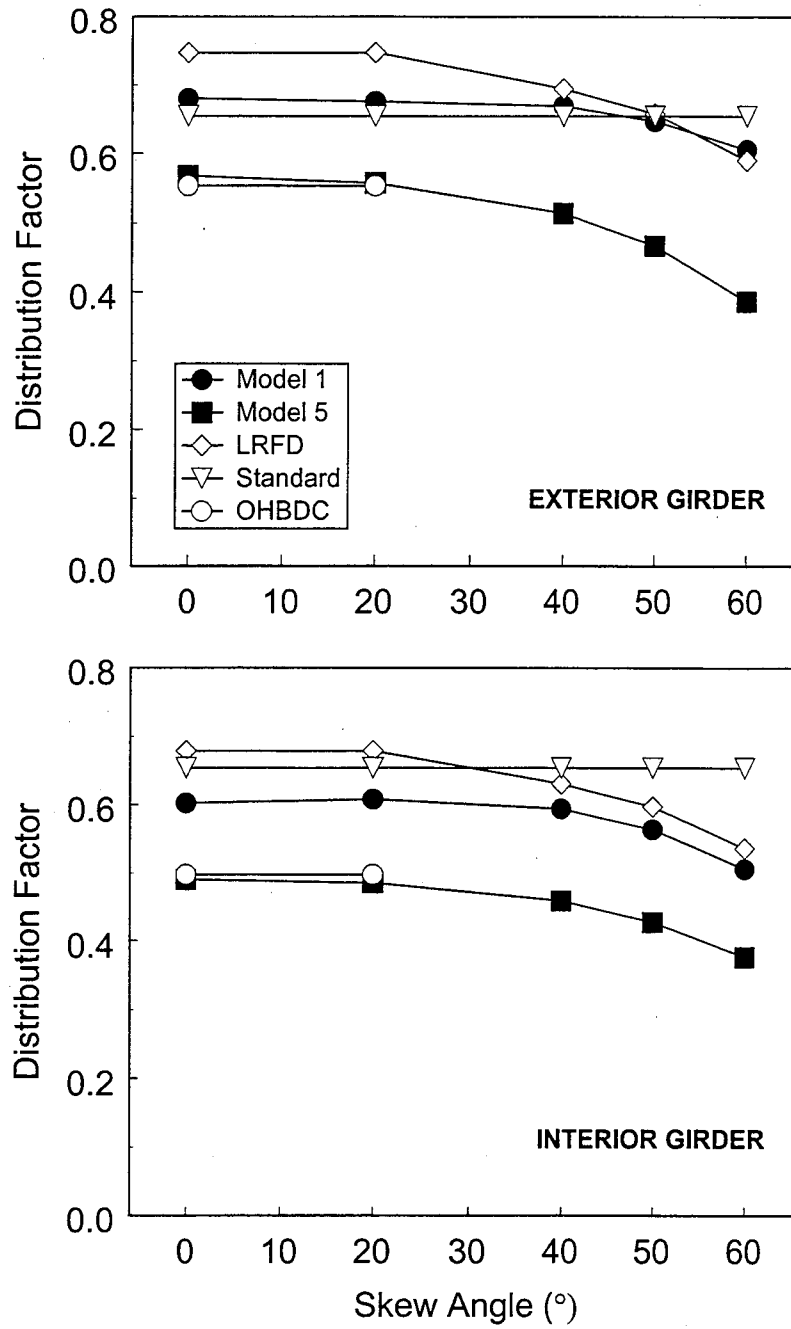


Figure 6.3. Distribution Factors for Truck Loading

#### 6.4.2 Effect of Lifts

Because the W74MG has such a wide top flange (Figure 3.3), the addition of a 3.75-inch lift to the model increased the effective thickness of the deck as well as causing a slight increase in composite girder stiffness. It is impossible to model the lift exactly, because its depth varied over the span. Nevertheless, the change leads to an increase in the ratio of lateral to longitudinal stiffness ( $D_x/D_y$ ) which in turn implies a more uniform distribution of girder moments and thus a lower live load distribution factor.

The difference between Models 1 and 2 was the presence of a lift between the top of the girder and the bottom of the deck. Figure 6.4 shows the distribution factors for Models 1 and 2 as the skew varies. The light symbols represent Model 1 and the dark symbols represent the model after the lift was added.

For the exterior girder, the addition of lifts caused a reduction in the live load distribution factor from 15 percent ( $0^\circ$  skew) to 21 percent ( $60^\circ$  skew). The reduction in distribution factor due to the presence of lifts was smaller for interior girders. This reduction ranged from 8 percent ( $0^\circ$  skew) to 18 percent ( $60^\circ$  skew).

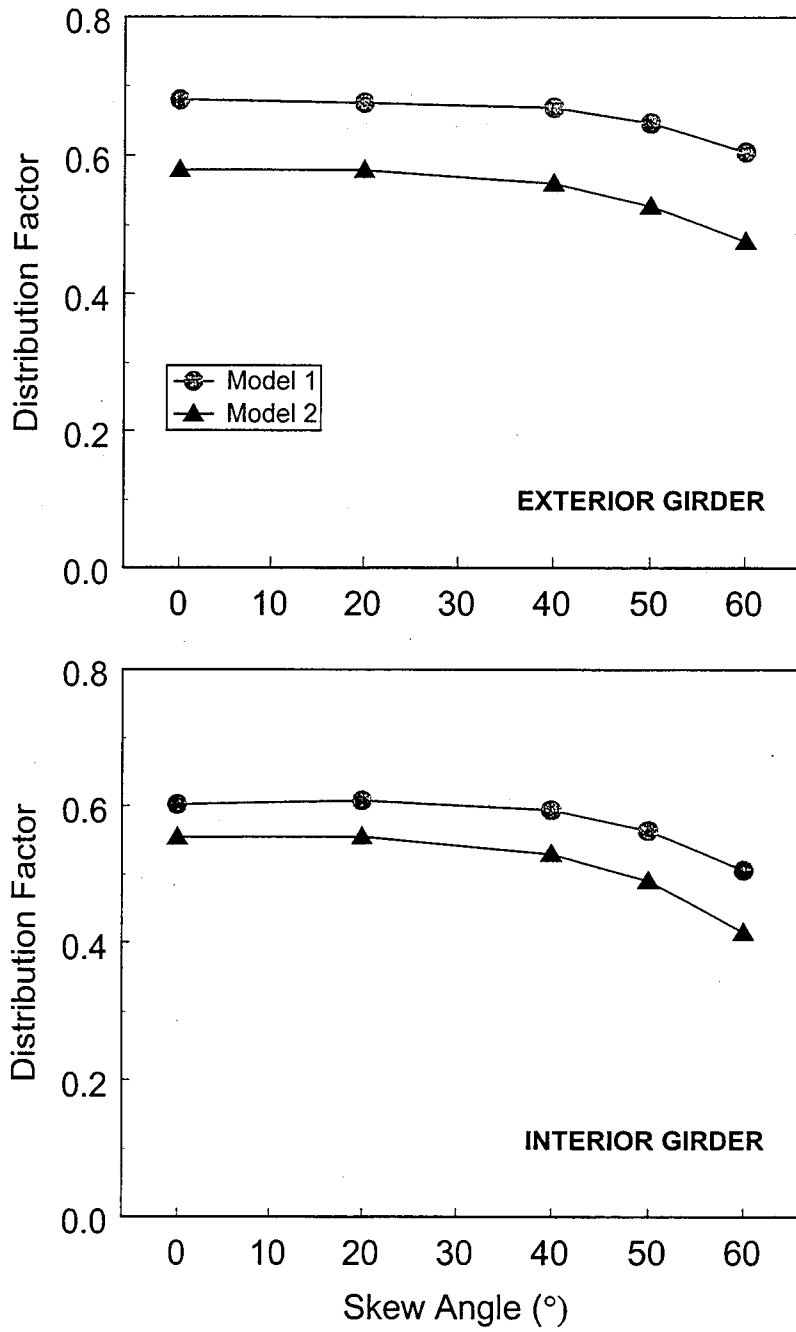


Figure 6.4. Effect of Lifts

### 6.4.3 Effect of Intermediate Diaphragms

The only difference between Models 2 and 3 was the addition of intermediate diaphragms in Model 3. Live load distribution factors for the two models are shown in Figure 6.5. The basic case (Model 2, no diaphragms) is shown using light symbols and the modified case (Model 2 with diaphragms) is shown using heavy symbols.

For both interior and exterior girders, the addition of intermediate diaphragms had less impact on the live load distribution factors than did any other variable investigated. This finding is in agreement with the conclusions of Gamble (1973), who found that intermediate diaphragms provided little benefit to the live load distribution factors.

For the exterior girders, the effect of adding intermediate diaphragms depends on skew. At low skew angles the intermediate diaphragms slightly increased the live load distribution factor and design moment, whereas at high skew angles ( $\geq 30^\circ$ ) the diaphragms were beneficial. The penalty imposed by adding intermediate diaphragms at low skew angles appears surprising but has also been observed by others (Stanton and Mattock, 1986; Gamble, 1973). The magnitude of the penalty appears to depend on the transverse location of the truck and its extreme position with respect to the exterior girder line

For the interior girders, the addition of intermediate diaphragms distributes the load more uniformly across the bridge. This uniform distribution reduced the live load distribution factors by an average of 3 percent.

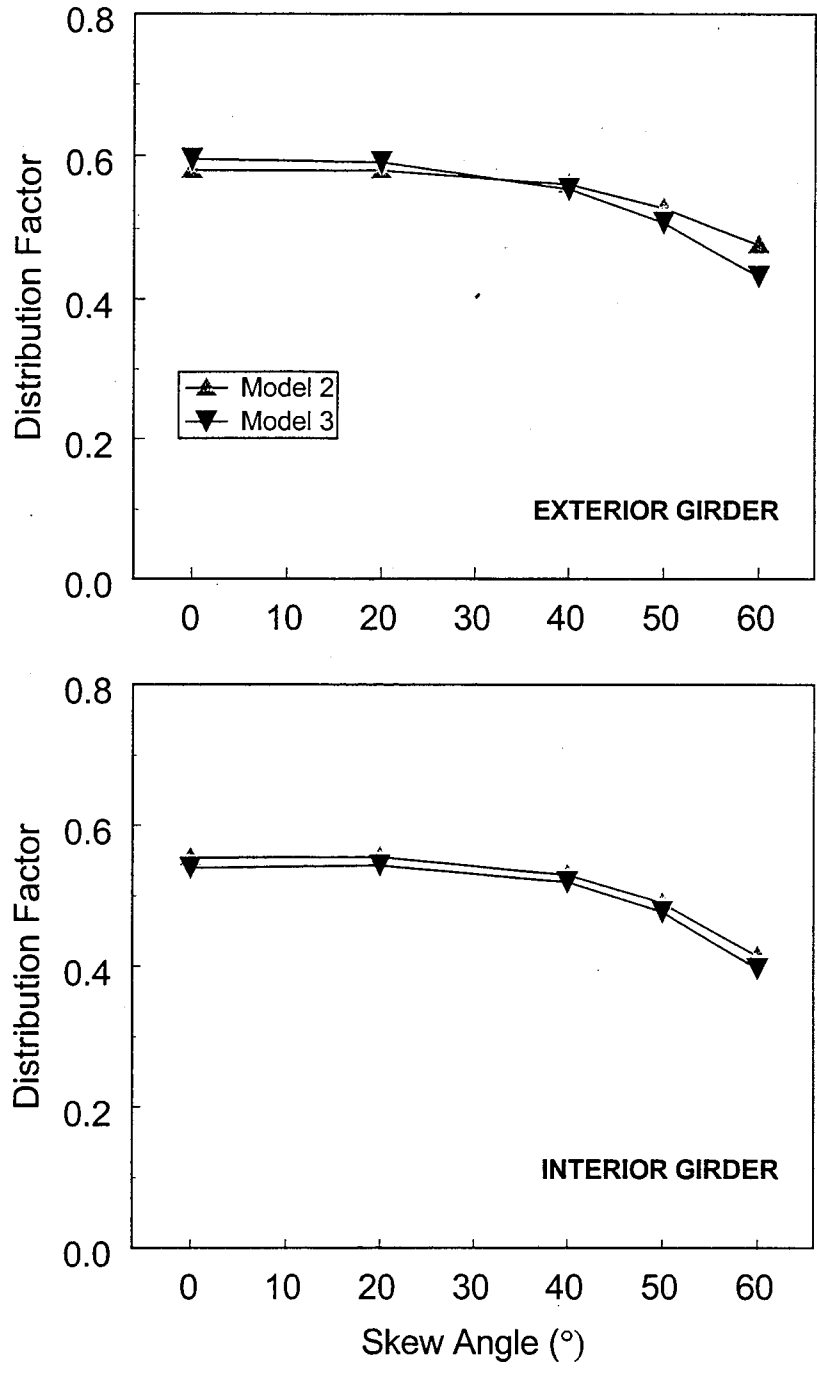


Figure 6.5. Effect of Intermediate Diaphragms

#### 6.4.4 Effect of End Diaphragms

The difference between Models 3 and 4 was the addition of end diaphragms. End diaphragms influence the midspan moment due to a single loaded girder in two ways. If the diaphragms are torsionally stiff, they inhibit end rotation of the loaded girder at the expense of causing some end rotation in the adjacent, unloaded, girders. The negative end moment so introduced in the loaded girder reduces the positive midspan moment. This behavior corresponds to a reduction in the live load distribution factors and occurs at all skew angles.

Midspan moments are reduced by the end diaphragms occurs a second way in skew bridges. It is illustrated by the simple model shown in Figure 6.6, in which the bridge superstructure is represented by a single beam element. The structure is free to rotate about an axis parallel to the abutments, which lie at an angle ( $90^\circ - \alpha$ ) to the longitudinal axis of the bridge. If a uniform load is applied to the superstructure, torsional and flexural end moments are induced. The flexural end moment, which is numerically equal to the reduction in midspan moment, is given by Equation 6.8. The reduction in midspan moment can be seen to increase with skew angle and with torsional stiffness of the bridge.

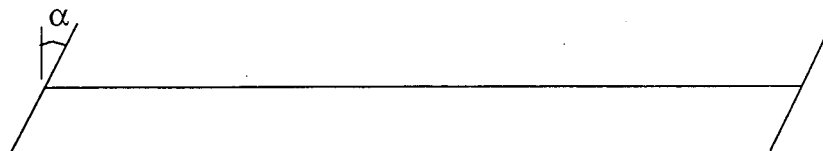


Figure 6.6. Fixed-Fixed Beam with a Skew Angle  $\alpha$

$$M_o = \frac{wl^2/12}{\left[ \frac{EI}{GJ} \cot^2 \alpha + 1 \right]} \quad (6.8)$$

where:  $M_o$  = reduction in midspan moment  
 $w$  = distributed load  
 $l$  = span length  
 $E$  = modulus of elasticity  
 $I$  = moment of inertia  
 $G$  = shear modulus of elasticity  
 $J$  = torsional moment of inertia

For the exterior girder, the addition of end diaphragms caused the distribution factors to decrease regardless of skew. The difference between Models 3 and 4 increased with increasing skew. This difference ranged from 6 percent at no skew to almost 23 percent when the skew angle was 60°.

The same trend was present for the interior girders. When the skew angle was small (0°), the difference between the distribution factors from the two models was less than 2 percent. As the skew angle increased to 60°, the difference increased to more than 24 percent.

Figure 6.7 shows the distribution factors for Models 3 and 4 as the skew angle varies.

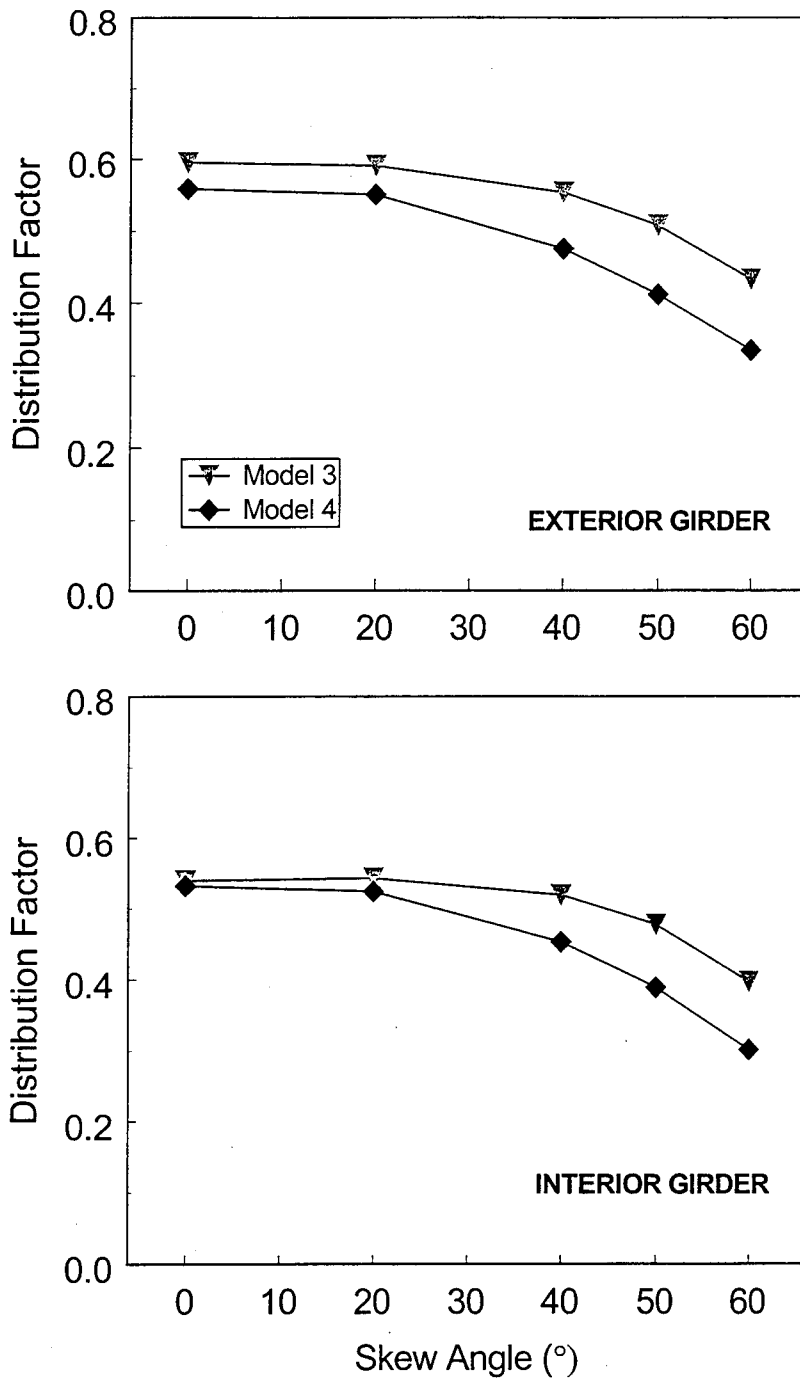


Figure 6.7. Effect of End Diaphragms

#### 6.4.5 Effect of Continuity

The difference between Models 4 and 5 was the addition of Spans 1 and 3 to create a 3-span continuous bridge. The addition of Spans 1 and 3 effectively increased the longitudinal stiffness of the bridge while the lateral stiffness of the bridge remained the same. Consequently the ratio of lateral to longitudinal stiffness ( $D_y/D_x$ ) decreases and the load distribution factor should be expected to increase.

Figure 6.8 shows the load distribution for Models 4 and 5 for a range of skew angles. The 1-span model (Model 4) is shown with light symbols while the 3-span continuous model (Model 5) is shown with dark symbols.

For the exterior girder, Model 5 produced distribution factors that were higher than those of the 1-span model (Model 4) regardless of skew. The difference between the two models was small (< 2 percent) at low skew angles but increased with skew.

For the interior girder, the difference between the predictions of the two models changed sign at 40° skew. The reason for this behavior is unknown.

Note that the continuity in the actual bridge might decrease if it were loaded to the code load level. Under the higher loads specified by LRFD, the slab might crack at the piers and the negative moment might be distributed to the adjacent spans.

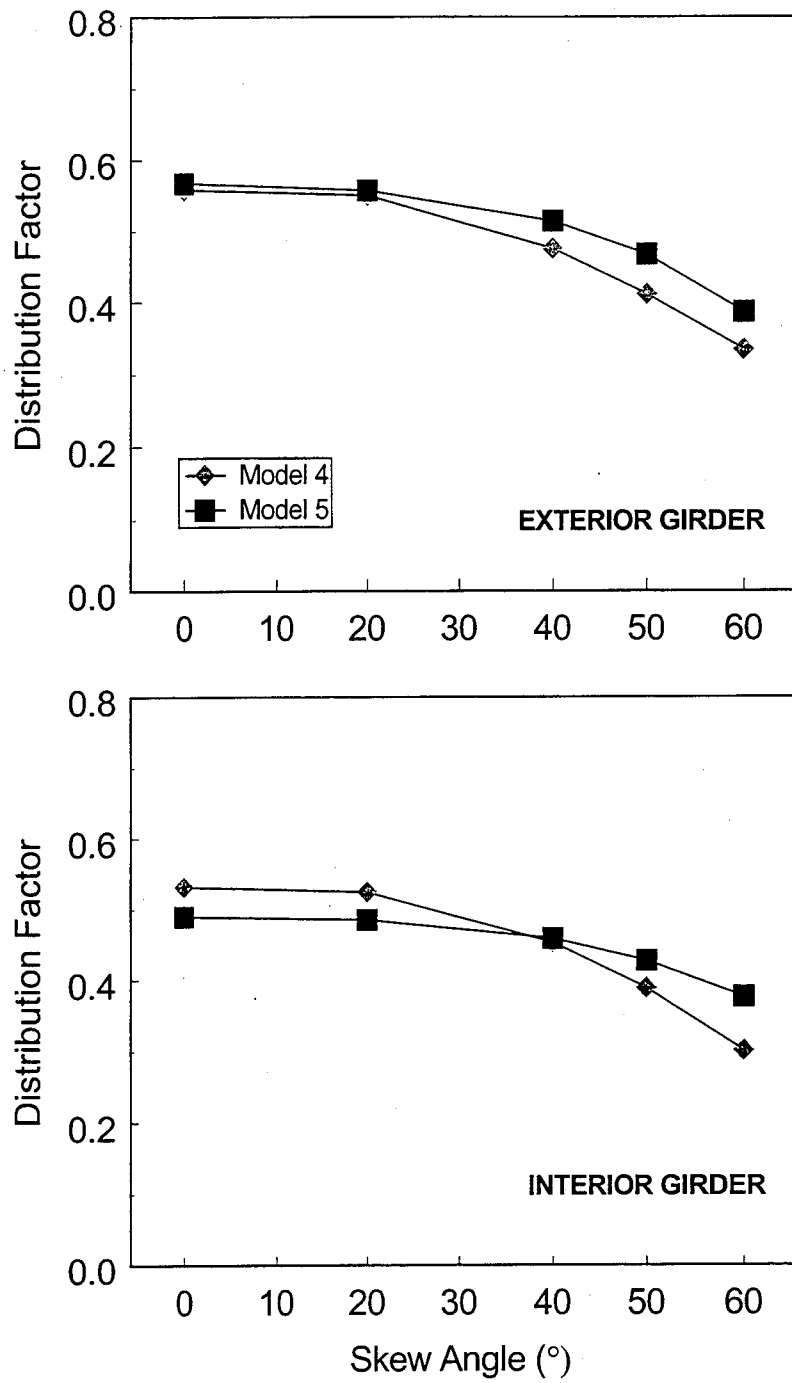


Figure 6.8. Effect of Continuity

#### 6.4.6 Comparison of Effects

Figure 6.9 shows the effect on the distribution factors due to the presence of lifts, intermediate diaphragms, end diaphragms and continuity. It summarizes the information shown in Figures 6.3 to 6.8, and expresses it in terms of change rather than absolute values. The distribution factors for Model 5 can be obtained as:

$$DF_5 = DF_1(1+\alpha_L)(1+\alpha_{ID})(1+\alpha_{ED})(1+\alpha_C)$$

where:

$DF_i$  = distribution factor for model  $i$

$\alpha_L$  = change in DF due to lift

$\alpha_{ID}$  = change in DF due to intermediate diaphragm

$\alpha_{ED}$  = change in DF due to end diaphragm

$\alpha_C$  = change in DF due to continuity

A summary of the findings is as follows:

- Regardless of skew, adding a lift significantly reduced the live load distribution factors for both the exterior and interior girders. This decrease in distribution factors ranged from 8 percent (interior girder, 0° skew) to 21 percent (exterior girder, 60°). The change is caused by the increase in transverse stiffness.
- The addition of intermediate diaphragms had the least effect of any parameters investigated. For the interior girders, the effect of intermediate diaphragms reduced the distribution factors slightly by nearly a constant amount (2.5 percent) regardless of skew. The effect on exterior girder was slightly larger, ranging from a 3 percent increase at no skew to a 9 percent decrease at 60° skew.
- For both interior and exterior girders, the addition of end diaphragms slightly decreased the distribution factors. The effect was least (less than 2 percent for interior girder, 0° skew) when the skew angle was small and became more

significant (more than 24 percent interior girder, 60° skew) as the skew angle increased.

- Continuity generally increased the distribution factors especially for large skew angles. The exterior girders showed almost no increase (<2 percent) for small skew angles but increased up to 13 percent for a 60° skew. The distribution factors for the interior girder were reduced for small skew angles (8 percent for no skew) and increased for large skew angles (25 percent for 60° skew).

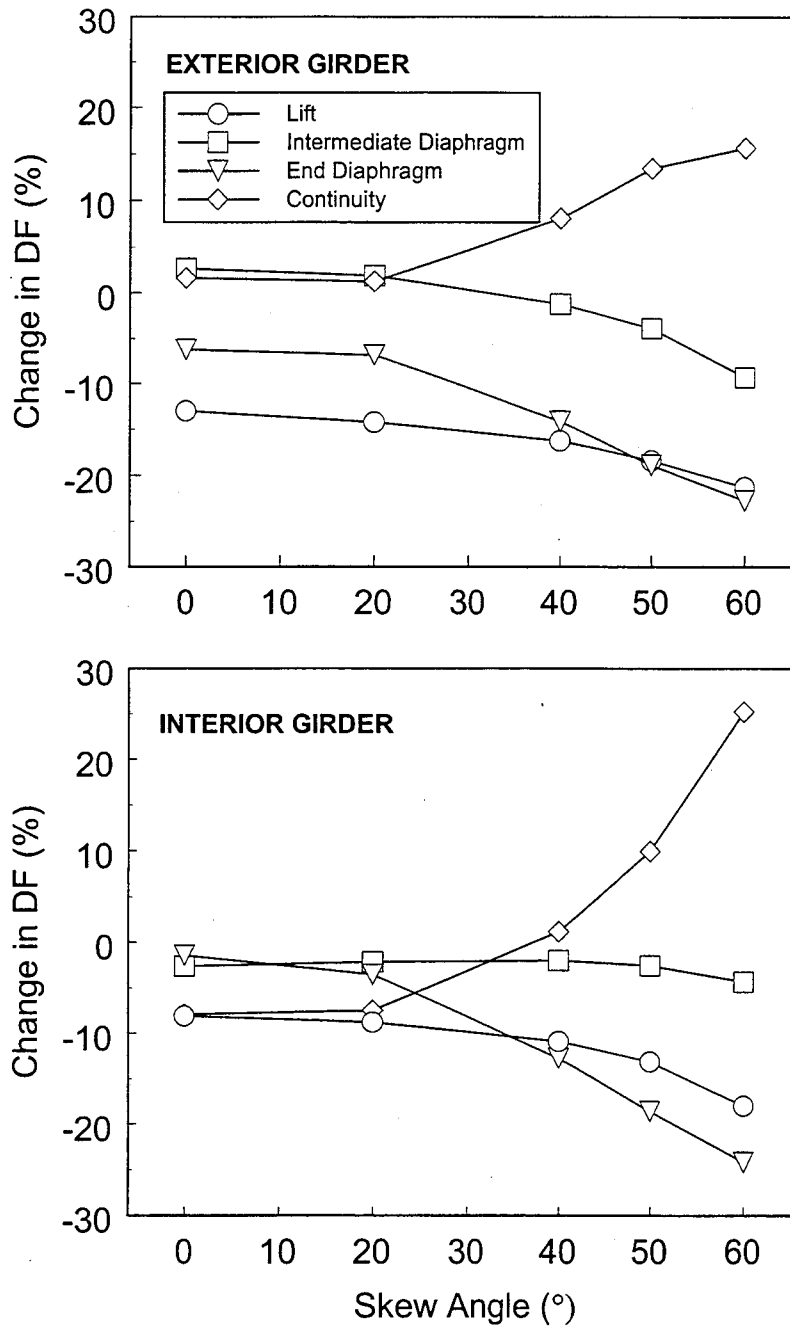


Figure 6.9. Combined Effects

#### *6.4.7 Effect of Skew*

A reduction in the distribution factor for a skewed bridge may occur because some of the wheels of the truck are closer to the supports than on right bridges. Another reason may be that, for skewed bridges, the slab will tend to bend along a direction perpendicular to the abutments. This behavior would transfer part of the truck load directly from the deck to the supports, instead of through the girder as in the case of a right bridge.

The ratio of distribution factor at any skew angle to the distribution factor at zero skew shows the effect of skew. Figure 6.10 shows the effect of skew for the five FE models as well as the effect of skew predicted by the AASHTO LRFD code.

For interior and exterior girders, skew decreased in distribution factors at large ( $>40^\circ$ ) skew angles. The distribution factors increased slightly ( $<2$  percent) for some of the models when the skew angle was  $20^\circ$ . This slight increase in distribution factors is consistent with previous research (Bishara et al., 1993). In general, interior girders were more affected by skew than exterior girders, however the opposite is true for the girders of Model 5.

Model 4 was influenced the most by the distribution factors. This result is likely due to the influence of the end diaphragms and skew discussed in Section 6.4.4. Model 1 was least effected by the skew angle out of the 5 FEM models.

With the exception of Model 4, the AASHTO LRFD Specifications closely predicted the effect of skew of the various models for the interior girders.

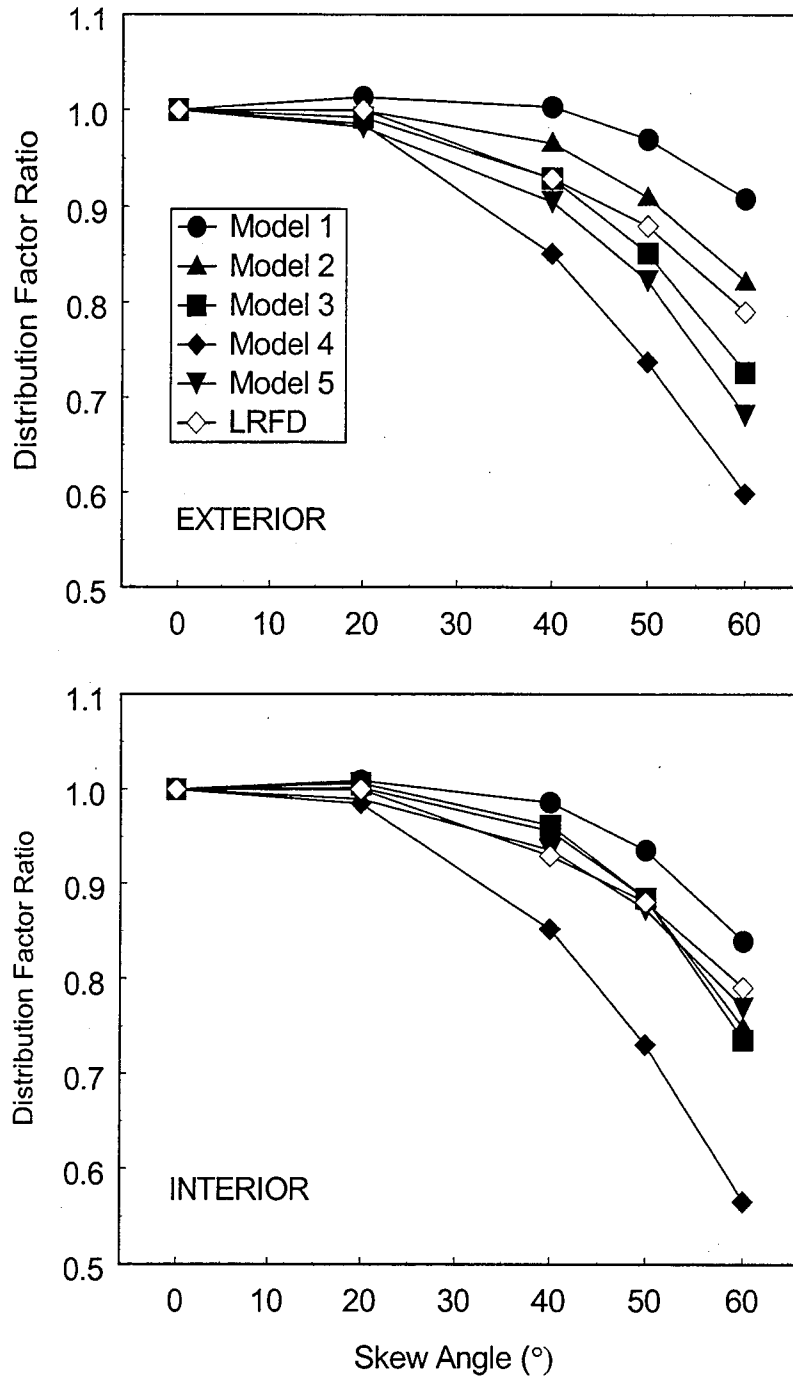


Figure 6.10. Effect of Skew

## 6.5 EVALUATION OF CODE LIVE LOAD DISTRIBUTION FACTORS – LANE LOADING

The girder design moment from the AASHTO LRFD code is based on truck plus lane loading. All of the codes studied provide only distribution factors for trucks, so those for lane loading are taken to be the same. For the SR18/SR516 overcrossing, the midspan moment due to lane load was two-thirds of the moment due to truck load, so a reduction in the lane load distribution factors could represent a significant savings. Figure 6.11 shows the distribution factors for the AASHTO truck and lane loading computed using finite element Models 1 and 5. As in Figures 6.4 to 6.8, the shapes of the symbols indicate the bridge geometry (Model 1 or 5). However, here solid symbols indicate truck loading and open symbols, lane loading. The conclusions for the lane load distribution factors are as follows:

- Distribution factors calculated due to lane loading are lower than those due to truck loading. This trend is consistent over all variables (skew, exterior/interior girders, model configuration).
- The FEM-based live load distribution factors for truck loading are already lower than the ones used in the AASHTO LRFD. The FEM based distribution factors for lane loading are lower still. Thus use of the AASHTO LRFD distribution factors to compute girder moments due to lane loading is conservative for the SR18/SR516 overcrossing.
- On average, the lane load distribution factor is 10 percent lower than that of the truck load distribution factors. The range is from 18 percent (exterior girder, Model 5, 60° skew) to 3 percent (interior girder, Model 1, 0° skew).

The conclusion that lane load leads to lower distribution factors than does truck loading is consistent with the findings of previous research (e.g., Stanton, 1992). That study addressed the distribution of concentrated loads among adjacent members in precast concrete floors. Stanton found that the distribution width for a uniform load was larger than that for a concentrated load.

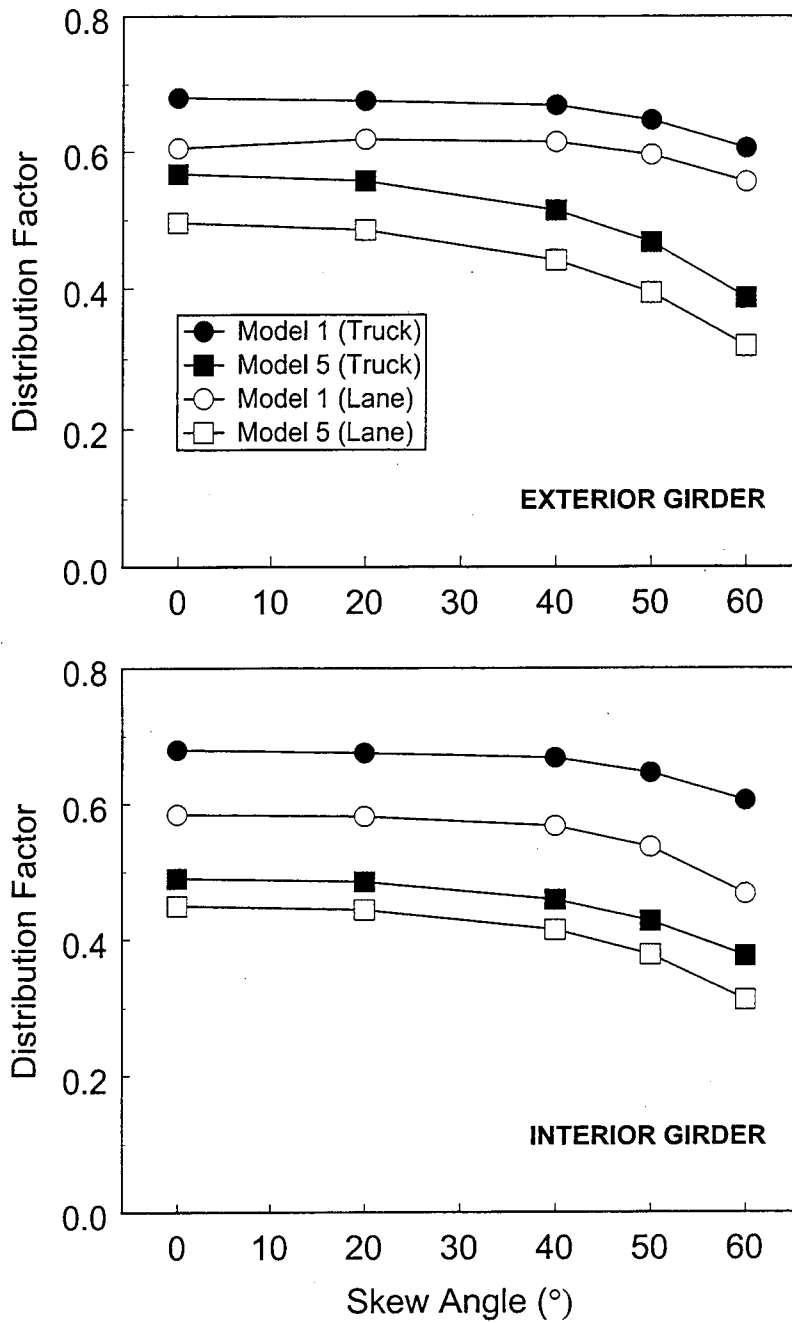


Figure 6.11. Distribution Factors for the AASHTO Truck and Lane Loading

## CHAPTER 7 DESIGN IMPLICATIONS

Chapter 7 investigates the consequence of using the live load distribution factors that were predicted by the AASHTO LRFD code as opposed to using those predicted by the FEM of the SR18/SR516 overcrossing. In addition, the individual effects of adding the lift, intermediate diaphragms, end diaphragms and continuity on the design of the precast prestressed concrete girder are investigated.

If the live load distribution factors that were calculated from the finite element study and verified by the live load test had been used in the design of the bridge, the number of strands and the release strength could have been reduced or the span could have been increased. In practice, the use of fewer strands would offer an additional benefit because prestress losses would diminish and would allow for even a greater reduction in the number of strands than was computed here.

A spreadsheet that is used by the WSDOT to design precast prestressed concrete girders in accordance to the AASHTO LRFD code was used to investigate the effect a change in distribution factors would have on the design properties of the girders. The same girder properties, prestress losses and design parameters that were used in the design of the girders were used in this investigation. The live load truck moment was found with Dr. Beam (1997). The exterior girder controlled the design of the SR18/SR516 overcrossing (having the larger distribution factor from the AASHTO LRFD code), and was therefore the only one investigated.

Figure 7.1 shows the effect that changing the distribution factors from the ones predicted from the AASHTO LRFD to those predicted from the FEMs would have on the

required initial concrete strength, number of strands and span. All the values were calculated with models having a 40° skew. The new values for release strength and number of strands were obtained while keeping the original span length (found using the AASHTO LRFD distribution factors). The release strength and number of strands were then kept as the original values (found using the AASHTO LRFD distribution factors) and the new span was calculated.

The lines starting at the far left of each figure represent the design parameters used in the girders as required by the AASHTO LRFD code. The lines at the far right are the design parameters using the finite element model of the SR18/SR516 overcrossing (Model 5) with different distribution factors for the truck and lane loading. Intermediate changes in the design parameters are due to the addition of the lift, intermediate diaphragms, end diaphragms and continuity using only the truck load distribution factors.

The design parameters using the distribution factors from the FEM of the SR18/SR516 overcrossing (Model 5) with different distribution factors for the truck and lane loading differed significantly from those obtained by using the distribution factors from the AASHTO LRFD code. If the distribution factors from the SR18/SR516 FEM had been used in the design of the girders, the required release strength could have been reduced from 51 MPa (7.4 ksi) to 44.0 MPa (6.4 ksi), and 4 fewer strands could have been used, alternatively the span could have been increased by 2.1 m (6.8 ft).

The design parameters using the AASHTO LRFD Specifications and Model 1 were nearly identical. This should be expected since the AASHTO LRFD equations predicting the distribution factors are based on FEMs similar to those of Model 1.

The addition of the lift, intermediate diaphragms and end diaphragms all cause a decrease in the release strength or number of strands or an increase in span length, while the addition of continuity had opposite effects on the factors. The largest changes in the design parameters came from the addition of the lift and end diaphragms. Smaller changes occurred due to the addition of continuity while almost no change occurred when intermediate diaphragms were added.

The difference in the design parameters could have been important for this particular bridge because the contractor had considerable difficulty achieving the required release strength of 51 MPa (7.4 ksi) fast enough to produce the girders on a 24-hour cycle. Reducing the release strength to 42.6 MPa would have greatly facilitated fabrication. For other bridges, the longer span capability increases the number of bridge configurations that can be considered, including the possibility of increasing traffic safety and reducing cost by eliminating piers. Longer spans are already available with the WSDOT's new 2100M and 2400M girders (Seguirant, 1998), but these are heavy enough that in many cases, they will have to be fabricated and transported in sections and post-tensioned on site. Extending the span capability of the lighter, one-piece, W74MG girder is likely to be simpler and more economical.

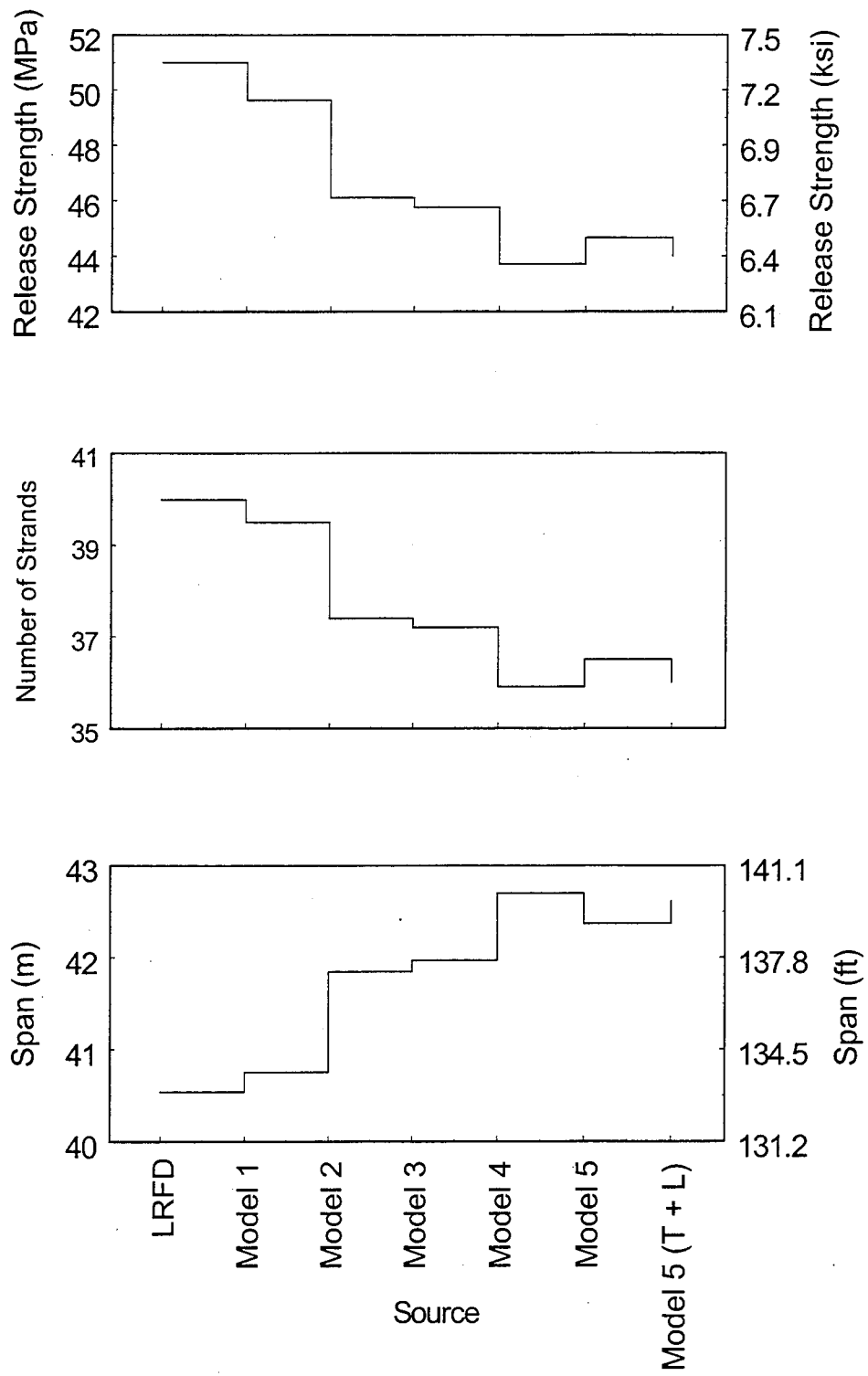


Figure 7.1. Design Implications for Live Load Distribution Factors

## CHAPTER 8 CONCLUSIONS AND RECOMMENDATIONS

This research project focused on evaluating the live load distribution factors for the SR18/SR516 overcrossing. A static live-load test was performed on the bridge. The results of the live-load test were analyzed and compared with the results from a finite element model of the bridge subjected to similar loading. Four additional sets of finite element models were developed in order to compare results with previous research and to determine the effect that the lifts, intermediate diaphragms, end diaphragms, continuity and skew angle had on the distribution factors. The AASHTO truck and lane loading was applied to the various models and the distribution factors were calculated. The distribution factors obtained from the finite element models were compared with the predicted distribution factors from several codes. This chapter summarizes the major findings and provides recommendations for future research.

### 8.1 STATIC LIVE-LOAD TEST

In general, the moments from the finite element model (Model 5) agreed closely with those calculated using the measured data. The FEM midspan moment was a little larger in almost all cases but was within 6 percent of the moment predicted from the SR18/SR516 FEM model for the moment directly under the load (Figure 5.2). The average difference was 16.8 kN-m (149 kip-in.), which corresponds to 1.4 microstrain. A good correlation between the finite element model predicts and the measured data also existed for girders adjacent to the loaded girders. It was concluded that the finite element model of the SR18/SR516 overcrossing reliably predicted the true behavior of the bridge.

## 8.2 COMPARISON WITH CODES

For the exterior and interior girders, Table 8.1 lists the ratio of live load distribution factors predicted by Model 5 to the factors for three codes for 40° skew, which was the skew angle for the SR18/SR516 overcrossing. A value smaller than one indicates a smaller distribution factor predicted by the FEM model. Although the OHBDC is only valid for skew angles less than 20 degrees, it is still shown here for comparison.

For the exterior girders, the largest error occurs in the AASHTO LRFD code predictions, while for interior girders, the AASHTO Standard gives the largest difference error. In all cases the OHBDC predictions are the closest, by a considerable margin.

**Table 8.1 Ratio of Model 5 and Code Distribution Factors**

Girder	AASHTO LRFD	AASHTO Standard	OHBDC
Exterior	0.74	0.79	0.94
Interior	0.73	0.70	0.92

Table 8.2 lists the ratio of distribution factors predicted by a simply supported model of Span 2 with only the deck and girders modeled (Model 1) and the three codes for a skew angle of 40°.

In general, the AASHTO LRFD code distribution factors are closer to the simply supported model (Model 1) than to the SR18/SR516 overcrossing model (Model 5) (Figure 6.3). This should not be surprising since the equations for the distribution factors in the AASHTO LRFD are based on research performed on simply supported models similar to Model 1. The distribution factors from the AASHTO LRFD code do a

particularly good job of predicting the distribution factors for Model 1 considering they are meant to be, on average, 5 percent conservative (Zokaie et al.,1991).

The AASHTO Standard Specification also closely predicts the distribution factors for Model 1 (Figure 6.3). The Standard Specification is slightly unconservative for the exterior girder and slightly conservative for the interior girders.

The OHBDC predicts distribution factors that are significantly smaller than those predicted with Model 1 for both exterior and interior girders (Figure 6.3).

**Table 8.2. Ratio of Model 1 and Code Distribution Factors**

Girder	AASHTO LRFD	AASHTO Standard	OHBDC
Exterior	0.97	1.03	1.22
Interior	0.94	1.09	1.18

### 8.3 INFLUENCES ON THE LIVE LOAD DISTRIBUTION FACTORS

The live load distribution factors were influenced when lifts, intermediate diaphragms, end diaphragms and continuity were added to the finite element model. The type of loading also influenced the magnitude of the distribution factors. This section describes the effect of each of these parameters.

#### 8.3.1 Effect of Lifts

Adding a lift to the finite element model significantly reduced the live load distribution factors for both the exterior and interior girders, regardless of skew (Figure 6.4). This decrease in distribution factors ranged from 8 percent (interior girder, 0° skew) to 21 percent (exterior girder, 60°).

### ***8.3.2 Effect of Intermediate Diaphragms***

The addition of intermediate diaphragms had the smallest effect on the distribution factors of any of the three parameters investigated. The intermediate diaphragms increased the distribution factors for the exterior girders slightly (3 percent) for skew angles less than 30 degrees. At skew angles greater than 30 degrees, the intermediate diaphragms gradually decreased the distribution factors for the exterior girders up to 9 percent at 60 degrees skew (Figure 6.5). For interior girders, the effect of intermediate diaphragms reduced the distribution factors slightly by nearly a constant amount (2.5 percent) regardless of skew.

### ***8.3.3 Effect of End Diaphragms***

The addition of end diaphragms reduced the distribution factors by 6.5 percent for the exterior girders when the skew was less than 20 degrees (Figure 6.7). This reduction gradually increased when skew angles became larger than 20 degrees up to 23 percent when the skew angle reached 60 degrees. For the interior girders, the end diaphragms only slightly reduced the distribution factor at zero skew, but increased to 24 percent when the skew angle was 60 degrees.

### ***8.3.4 Effect of Continuity***

For the exterior girder, the addition of continuity produced distribution factors that were higher than those calculated when continuity was not included (Figure 6.8). The difference between the two models was small (< 2 percent) at low skew angles but increased to as large as 18 percent when the skew was 60°.

For the interior girder, the difference between the predictions of the two models changed sign at 40° skew. When the skew angle was less than 40°, the distribution factors was smaller when continuity was added. The reason for this behavior is unknown.

### ***8.3.5 Effect of Skew***

For interior and exterior girders, the effect of skew caused a decrease in the distribution factors at large (>40°) skew angles (Figure 6.10). In general, interior girders were more effected by skew than exterior girders, however the opposite is true for the girders of Model 5.

Model 4 was influenced the most by the distribution factors. This is likely due to the influence of the end diaphragms and skew discussed in Section 6.4.4. Model 1 was least affected by the skew angle out of the 5 FEM models.

On average, the AASHTO LRFD closely predicted the effect of skew for the interior girders (Section 6.4.7).

### ***8.3.6 Effect of Lane Loading***

The conclusions for the lane load distribution factors are as follows (Figure 6.11):

- Distribution factors calculated due to lane loading are lower than those due to truck loading. This trend is consistent over all variables (skew, exterior/interior girders, model configuration).
- The FEM based live load distribution factors for truck loading are already lower than the ones used in the AASHTO LRFD. The FEM-based distribution factors for lane loading are lower still.

- On average, the lane load distribution factor is 10 percent lower than that of the truck load distribution factors. The range is from 18 percent (exterior girder, Model 5, 60° skew) to 3 percent (interior girder, Model 1, 0° skew).

#### **8.4 DESIGN IMPLICATIONS**

The required release strength, number of strands and span length using the distribution factors from the FEM model of the SR18/SR516 overcrossing differed significantly from those obtained by using the distribution factors from the AASHTO LRFD code. If the distribution factors from the SR18/SR516 FEM had been used in the design of the girders, the required release strength could have been reduced from 51 MPa (7.4 ksi) to 44.0 MPa (6.4 ksi), and 4 fewer strands could have been used, alternatively the span could have been increased by 2.1 m (6.8 ft) (Figure 7.1).

#### **8.5 RESEARCH RECOMMENDATIONS**

Further research needs to be done on the distribution factors of long span precast prestressed concrete girder bridges. Important topics not addressed in this study include bridge width and girder spacing. A reduction in the live-load distribution factors would be especially relevant with the increasing use of high performance concrete when designers are trying to increase span lengths or reduce the initial required concrete strength.

Additional experimental work on other bridges should be done to verify the effect of lifts, intermediate diaphragms, end diaphragms and continuity.

## REFERENCES

- American Association of State Highway and Transportation Officials (AASHTO). (1994). *LRFD Bridge Design Specifications*, 1<sup>st</sup> Edition, Washington, D.C.
- American Association of State Highway and Transportation Officials (AASHTO). (1996) *Standard Specifications for Highway Bridges*, 16<sup>th</sup> Edition, Washington, D.C.
- Aswad, G., and Chen, Y. (1994). "Impact of LRFD Specification on Load Distribution of Prestressed Concrete Girders." *PCI J.*, 39(5), 78-89.
- Bakht, B., Jaeger, L. G. (1985). *Bridge Analysis Simplified*. McGraw Hill.
- Barr, P., Fekete, E., Eberhard, M., Stanton, J., Khalaghi, B. and Hsieh, J. C. (1998). "High Performance Concrete in Washington State SR18/SR516 Overcrossing." Washington State Department of Transportation Bridge and Structures Office, report, Olympia, Washington.
- Bishara, A. G., Liu, M. C., and El-Ali, N. D. (1993). "Wheel Load Distribution on Simply Supported Skew I-Beam Composite Bridges." *J. Struct. Engrg.*, ASCE, 119(2), 399-419.
- Chen, Y., and Aswad, A. (1996). "Stretching Span Capability of Prestressed Concrete Bridges under AASHTO LRFD." *J. Bridge Engrg.*, ASCE, 1(3),112-120.
- Dr. Beam, *Manipulation Structural Modeling Software*. (1997). Dr. Software LLC., Seattle, Wash.
- Ebeido, T., and Kennedy, J. B. (1996). "Girder Moments in Continuous Skew Composite Bridges." *J. Bridge Engrg.*, ASCE, 1(1),37-45.
- Goodspeed, C. H., Vanikar, S., and Cook, R. A. (1996). "High-Performance Concrete Definition for Highway Structures." *Concrete International.*, 18(2),62-67.
- Khaleel, M. A. and Itani, R. Y. (1990). "Live-Load Moments for Continuous Skew Bridges." *J. Struct. Engrg.*, 116(9), 2361-2373.
- Lin, C. S. and VanHorn, D. A. (1968). "The Effect of Midspan Diaphragms on Load Distribution in a Prestressed Concrete Box-Beam Bridge-Philadelphia Bridge." *Fritz Engrg. Lab. Rep. No. 315.6*, Lehigh Univ., Bethlehem, Pa.
- Mabsout, M. E., Tarhini, K. M., Frederick, G. R. and Tayar, C. (1997). "Finite-Element Analysis of Steel Girder Highway Bridges." *J. Bridge Engrg.*, ASCE, 2(3),83-87.

- Newmark, N. M., Siess, C. P., and Peckham, R. R. (1948). "Studies of Slab and Beam Highway Bridges, Part-I test of Simple-Span Right I-Beam Bridges." University of Illinois, Engineering Experiment Station, *Bulletin Series No. 375*.
- Ontario Ministry of Transportation and Communication (OMTC). (1992). *Ontario Highway Bridge Design Code*, 3<sup>rd</sup> Ed., Highway Engineering Division, Downsview, Ontario.
- SAP2000, *Integrated Finite Element Analysis and Design of Structures*. (1997). Computers and Structures Inc., Berkeley, Calif.
- Seguirant, S. J. (1998). "New Deep WSDOT Standard Sections Extend Spans of Prestressed Concrete Girders." *Prestressed Concrete Institute Journal*, 43(4), July-August, 92-119.
- Sithichai kasem, S. and W. L. Gamble. (1971). "Effect of Diaphragms in Bridges with Prestressed Concrete I-Section Girders." Civil Engineering Studies, *Structural Research Series No. 383*, Department of Civil Engineering, University of Illinois, Urbana.
- Stanton, J. F. and Mattock, A. H. (1986). "Load Distribution and Connection Design for Precast Stemmed Multibeam Bridge Superstructures." *NCHRP Report 287*.
- Stanton, J. F. (1992). "Response of Hollow-Core Slab Floors to Concentrated Loads." *Prestressed Concrete Institute Journal*, 37(4), July-August, 98-113.
- Westergaard, H. M. (1930). "Computations of Stresses in Bridge Slabs due to Wheel Loads." *Public Roads*, March, 1-23.
- Zokaie, T., Osterkamp, T. A., and Imbsen, R. A. (1991). "Distribution of Wheel Loads on Highway Bridges." *NCHRP Proj. Rep. 12-26*, Transp. Res. Board, Washington, D.C.

